MINIMUM WEIGHT DESIGN OF SYMMETRICALLY STIFFENED ORTHOTROPIC CYLINDERS UNDER AXIAL COMPRESSION

George Gerard

C. Lakshmikantham

Technical Report No. 292-2

30 March 1966

Prepared For

Contract No. NASw-1174
National Aeronautics and Space Administration
Washington 25, D. C.

ALLIED RESEARCH ASSOCIATES, INC.
VIRGINIA ROAD · CONCORD, MASSACHUSETTS

Summary

24983

The historical development and current status of compressive orthotropic stability theory is reviewed and a systematic development of the linear theory is presented. Available test data on orthotropically stiffened cylinders are synthesized and correlated in terms of this theory. The correlation was used to establish regions in which linear orthotropic theory appears to be valid in terms of currently available test data.

Within the restriction that the minimum weight analysis be confined to those regions where linear stability theory is valid, a generalized presentation for symmetrically stiffened orthotropic cylinders under compression was developed. Similarities and differences in the minimum weight behavior of stiffened cylindrical shells and flat transversely stiffened wide columns were investigated in some detail to provide a satisfactory physical picture. The concluding results provide a comparative evaluation of various forms of stiffening systems for cylindrical shells under compression.

Symbols

A_r		rib area
B_1		membrane axial rigidity in longitudinal direction
B_2		membrane axial rigidity in circumferential direction
B_3		membrane shear rigidity (average)
C		structural efficiency coefficient
d		cylinder diameter
D_1		bending ridigity in longitudinal direction
D_2		bending rigidity in circumferential direction
D_3		twisting rigidity (average)
E		elastic modulus
h		rib height
k_a	$= B_2/B_1$	
k_x		cylinder buckling coefficient
K		spring constant
L		length
L_t		support spacing
m		number of half-wavelengths in longitudinal direction, also exponent
n		number of half-wavelengths in circumferential direction, also exponent
N		axial load per unit width
R		cylinder radius
$\bar{t}$		effective thickness
t_s		cylinder wall thickness
t_1		area of sheet and stiffener per unit width in a plane perpendicular to the circumferential direction
t_2		area of sheet and stiffener per unit width in a plane perpendicular to the longitudinal direction

Symbols (Continued)

U	asymmetric m-continuous buckling
w	lateral deflection
w_o	stiffener width
X	wavelength parameter
Z_x	curvature parameter
α	$= B_1D_2/B_2D_1$
α_p	stiffened wide column efficiency coefficient
β, $\overline{\beta}$	wavelength parameters
γ, δ	orthotropic parameters
λ	half wavelength in axial direction
ν	Poisson's ratio
Σ	solidity
σ_{exp}	experimental buckling stress
σ_o	optimum stress for stiffened wide columns
σ_x	theoretical buckling stress

MINIMUM WEIGHT DESIGN OF SYMMETRICALLY STIFFENED ORTHOTROPIC CYLINDERS UNDER AXIAL COMPRESSION

1. Introduction

Minimum weight analysis of stiffened cylindrical shells under compressive loading is of fundamental interest in the structural design of launch and space vehicles. Unfortunately, cylindrical shells under compression are probably the least reliable of all structural components that can be designed because of discrepancies which may exist between linear stability theory and the scatter of experimental data. This situation is poorest for isotropic cylinders which exhibit an unusually high sensitivity to imperfections; it can improve dramatically depending upon the type of stiffening system employed, however.

Thus, in contrast to the general acceptance of minimum weight analyses of flat plate elements which are based upon a satisfactory correlation of local and general instability theory with experiments, existing minimum weight analyses of cylindrical shells under compression are somewhat suspect and should be used with some caution. This conclusion is based upon the fairly comprehensive review of available minimum weight literature contained in Ref. 1.

The basic requirement for acceptance of minimum weight theory is clearly satisfactory agreement between experiments and theory for the basic instability modes. Fortunately, recent progress of a theoretical and experimental nature on stiffened cylindrical shells under compression has permitted a clearer understanding of the conditions under which satisfactory agreement between theory and experiment can be achieved. Thus, for the purpose of defining the current status of theory and test data in this area, a comprehensive review of linear orthotropically stiffened shell theory is presented herein and available test data are evaluated consistently in terms of this theory. A synthesis of these test data are presented in Section 2 which provides a tentative indication of the regions in which linear orthotropic stability theory is satisfactory.

In Section 3, the basic approach and assumptions involved in constructing a general theory for the minimum weight design of symmetrically stiffened orthotropic cylinders under axial compression is presented. Similarities and differences

between the minimum weight design of flat, transversely supported, longitudinally stiffened panels and the frame supported, cylindrical shell counterparts are investigated in some detail in order to arrive at a satisfactory physical picture of the minimum weight behavior of cylindrical shells.

Fundamental design synthesis results concerning the relative efficiencies of various types of minimum weight stiffening systems for cylindrical shells are presented in Section 4. These results include only those regions where linear orthotropic theory and test data correlate although the theory is sufficiently general to accommodate changes in the regions as they become better defined. Major conclusions drawn from a comparative evaluation of these results are presented in Section 5.

2. Assessment of Linear Orthotropic Stability Theory

Historical Review of Theoretical Developments

The historical development of the general compressive instability theory of stiffened cylindrical shells is marked by two periods of activity; the early and mid 1930's which marked the introduction of semimonocoque metal construction in aircraft and a current one, roughly a decade old, motivated by the design of launch and space vehicles.

The early theoretical investigations were performed by Flügge,[2] Dschou[3] and Taylor.[4] Flügge derived a set of three linear coupled equilibrium equations analogous to those used by investigators of isotropic cylinders at that time. Dschou solved these equations for stiffened circular cylinders under axial compression. Taylor utilized the Donnell assumptions for cylindrical shells and succeeded in deriving a single uncoupled eighth order equilibrium equation for orthotropic shells which reduced to Donnell's equation for an isotropic cylinder. The Taylor-Donnell type of equation has generally been used in all subsequent work.

The fact that this theory was used for comparison with experimental data with little success[5] in 1943, as well as almost a complete preoccupation with isotropic cylinders under compression since that time has produced the unfortunate result that the early work languished. Becker[6, 7] and Becker and Gerard[8] reviewed this situation in the late 1950's and concluded that orthotropic general instability theory for compressed cylinders had never been confronted previously with test data in which local instabilities had not preceeded failure. On the basis of more modern test data on external pressure and torsion as well as one recent test in compression, they concluded that linear orthotropic theory may indeed be useful.[8] In addition, the theoretical work contained in Refs. 7 and 8 provided explicit elastic general instability solutions in the moderate length range for circumferentially and axially stiffened cylinders under a variety of loadings as well as results for the flat plate and short cylinder regions.

While all the preceding theory was concerned with the linear buckling load, Thielemann[9] developed a non-linear post-buckling deflection theory for orthotropic shells under a variety of loadings. The results obtained for ring and longitudinally stiffened cylinders under compression are particularly helpful in providing an understanding of the conditions where linear theory may be satisfactory.

Gerard[10] extended the previous work to derive a general set of equations for plastic general instability of geometrically orthotropic shells. These equations were used to derive plasticity reduction factors for a variety of loadings. The compressive loading case is of particular interest since the buckling loads for the axisymmetric and asymmetric modes are generally different when the cylinder is plastic or orthotropically elastic. In contrast, for the isotropic elastic cylinder, both modes result in the same buckling load. The influence of the buckling modes was studied in some detail in Ref. 11 and served to indicate the importance of utilizing the appropriate buckling mode for the compressive loading case.

Returning to post-buckling theory, Almroth[12] has utilized Thielemann's theory in combination with more extended post-buckling deflection functions to obtain a wide range of theoretical results for the minimum post-buckling load. In an important extension of linear buckling theory, DeLuzio et al[13] have presented a theory which includes prebuckling deformations of the orthotropic shell as well as the effects of stiffener location upon the buckling load. More recently, Block et al[14] have contributed a theory for stiffener asymmetry.

A development of linear stability theory has been the recent discovery[15, 16] that a previously unsuspected asymmetric buckling mode may govern for certain types of longitudinally stiffened cylinders. This mode is in good agreement with available test data and will be discussed in greater detail subsequently.

Linear Orthotropic Stability Theory

Having set an historical frame of reference, it is important now to review the essential assumptions and features of current linear orthotropic stability theory and to provide results that can be checked against test data. For this purpose, Appendix 1 contains a rather general formulation of orthotropic shell theory for symmetrical stiffening systems and its systematic reduction in terms of various constitutive relationships. Appendix 2 presents specific solutions for the compression and bending cases. In the interests of providing the essential theoretical results for correlation with available test data, the following summary of the compression case is presented here.

In Ref. 11, a solution for the general instability of orthotropic cylinders under axial compression was obtained on the basis that for moderate length cylinders, the number of buckles along the axis of the cylinder m, was large enough that it could be treated as a continuous parameter along with β, the ratio of the buckle length in the axial direction to that in the circumferential direction. The buckling

coefficient k_x, was treated as a function of two variables m and β for obtaining a minimum value. From the requirements of stationariness, the following quadratic equation was obtained for $\overline{\beta}^2$ in terms of the orthotropicity parameters γ, α, and δ and exclusive of Z_x, the curvature parameter.

$$\overline{\beta}^2 = \frac{\delta}{2}\left\{\frac{1-\alpha}{\alpha-\gamma} \pm \left[\left(\frac{1-\alpha}{\alpha-\gamma}\right)^2 + \frac{4}{\delta}\frac{1-\gamma}{\alpha-\gamma}\right]^{1/2}\right\} \tag{1}$$

where:
$$\alpha = B_1D_2/B_2D_1$$
$$\gamma = [(D_3/D_1)(1-\nu) + (\nu/2)(1+D_2/D_1)]\,[(B_2/B_3)(1+\nu) - (\nu/2)(1+B_2/B_1)]^{-1}$$
$$\delta = B_2\,[B_1\{(B_2/B_3)(1+\nu) - (\nu/2)(1+B_2/B_1)\}^2]^{-1}$$
$$\overline{\beta}^2 = B_2\,[B_1\{(B_2/B_3)(1+\nu) - (\nu/2)(1+B_2/B_1)\}]^{-1}\beta^2$$
$$\beta = nL/m\pi R$$

The corresponding buckling coefficient solution for moderate length orthotropic cylinders was given as

$$k_x = 0.702\,(1-\nu^2)^{1/2}\,Z_x U \tag{2}$$

where:
$$k_x = N_x L^2/\pi^2 D_1$$
$$Z_x = B_2 L^4/12\,R^2 D_1$$
$$U = 1;\ \text{axisymmetric mode}$$
$$= [(\alpha\overline{\beta}^2+\gamma)/(\overline{\beta}^2+1)]^{1/2};\ \text{asymmetric mode}$$

As a consequence of Eq. (1), it was found for certain combinations of γ, α and δ that β was imaginary. Hence, for these γ, α and δ combinations the moderate length asymmetric solution or more precisely m-continuous solution, did not apply. However, since the axisymmetric solution was independent of γ, α, δ and β, it was assumed that the axisymmetric solution prevailed in the regions where the moderate length solution failed. These conclusions, based upon the quadratic equation, are shown in Fig. 1. Zones II and V represent the combinations of γ and α for which the quadratic equation yields imaginary values for β. This figure also indicates that the axisymmetric solution governs in the region bounded by

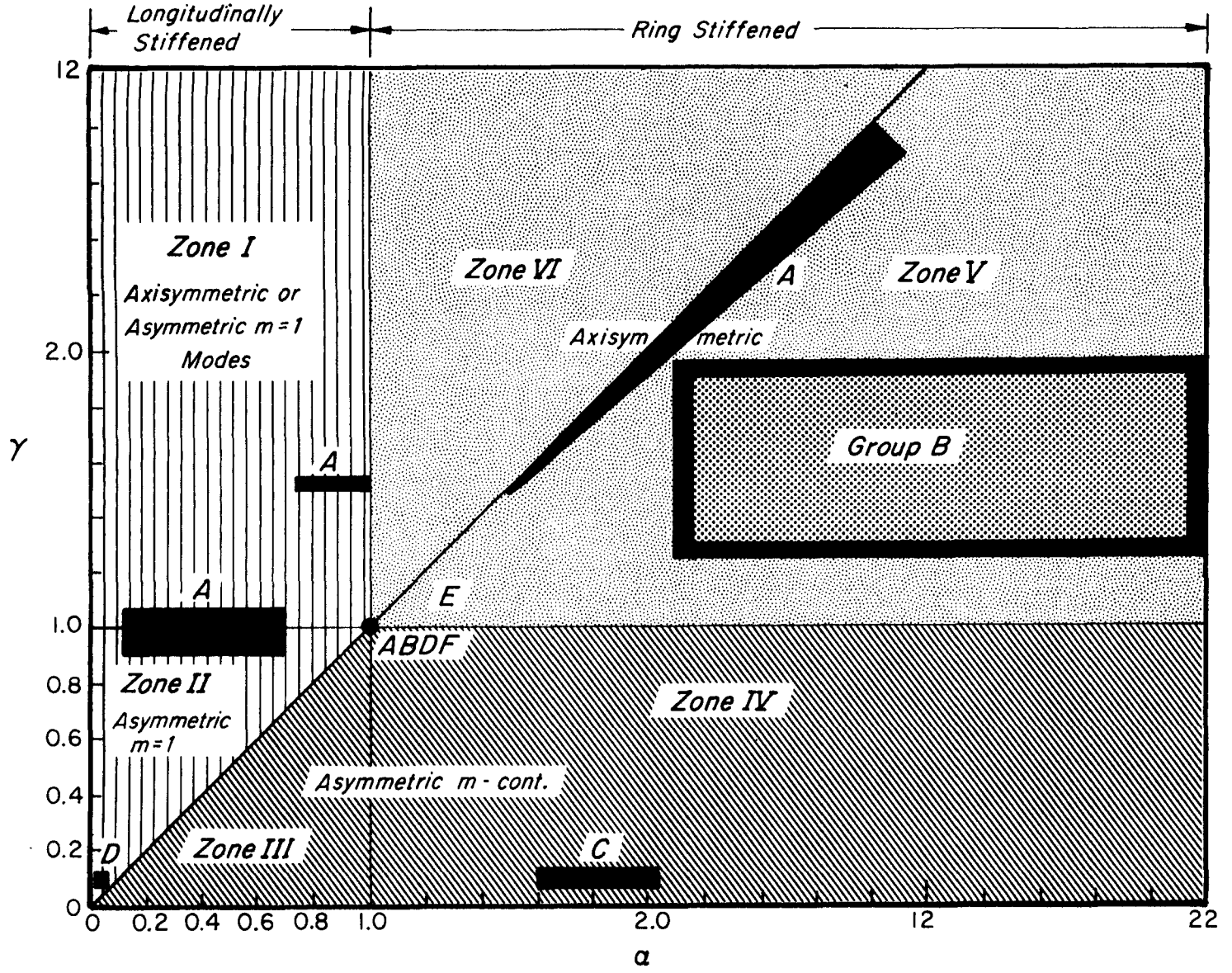

Figure 1 Governing buckling modes in various zones for orthotropic cylinders under compression. Also shown are regions A-F in which test data are available.

$\gamma \geq 1$, Zones I and VI, since the asymmetric m-continuous solution yields higher values in these zones.

During the course of the investigation reported in Ref. 15, it was found that in Zones I and II, an asymmetric solution with real β values can be obtained that is lower than the axisymmetric solution provided m were not treated as a continuous variable but were assigned the value m=1. By utilizing the nomenclature associated with Eq. (1), we can rewrite Eq. (11) of Ref. 11 with m=1 to obtain the following solution corresponding to the m=1 asymmetric mode:

$$k_x = 1 + 2\gamma(\bar{\beta}^4/\delta) + \alpha(\bar{\beta}^4/\delta) + (12Z_x^2(1-\nu^2)/\pi^4)\,[1+2(\bar{\beta}^2/\delta) + (\bar{\beta}^4/\delta)]^{-1} \tag{3}$$

By differentiating k_x with respect to $\bar{\beta}^2$ where now m=1, we obtain for the stationariness of k_x, the following expression for Z_x

$$[12(1-\nu^2)/\pi^4]Z_x^2 = [1 + 2(\bar{\beta}^2/\delta) + (\bar{\beta}^4/\delta)]^2\,(\gamma+\alpha\bar{\beta}^2)\,(1+\bar{\beta}^2)^{-1} \tag{4}$$

Finally, by substituting Eq. (4) into (3), we obtain the stationary value,

$$k_x = 1 + 2\gamma(\bar{\beta}^2/\delta) + \alpha(\bar{\beta}^4/\delta) + [1 + 2(\bar{\beta}^2/\delta) + (\bar{\beta}^4/\delta)]\;\;(\gamma+\alpha\bar{\beta}^2)\,(1+\bar{\beta}^2)^{-1} \tag{5}$$

Eqs. (4) and (5) constitute the basic equations for the asymmetric m=1 solution. For a cylinder with specified α, γ, δ; k_x and the corresponding Z_x can be found by assuming values of $\bar{\beta}$ and solving Eqs. (4) and (5). Typical results obtained for Zones I and II are presented in Ref. 15 and are compared with the axisymmetric solution and also the asymmetric solution with m-continuous. It was observed that the m=1 solution always results in lower values of k_x in Zone II. Typical results obtained in Zone I indicate that for $\gamma > 1$, the asymmetric m=1 solution is above the axisymmetric solution and then falls below at a value of Z_x that depends upon γ. Thus, either solution can apply in this region. Fig. 1 illustrates and summarizes the buckling modes which apply in each zone.

Correlation of Theory and Test Data

As indicated in Refs. 8 and 16, correlation of test data on cylinders designed specifically to check orthotropic theory is excellent for hydrostatic pressure and torsion loadings. Similarly, test data contained in Refs. 16, 17 and 18 on specially designed and fabricated stiffened test cylinders under axial compression and also bending are in suprisingly good agreement with the predictions of linear orthotropic general stability theory.

The range of orthotropic variables covered by the test data of Refs. 16, 17 and 18 are shown as Groups A and B respectively in Fig. 1. Also shown as Group C are test results on filament wound cylinders[19] analyzed in Ref. 15. It can be observed that it is desirable to cover a far broader range of variables than represented by these three groups to assess the complete accuracy of the orthotropic theory. Consequently, a search was initiated for test cylinders which could be considered to be in the orthotropic category by virtue of their stiffening arrangement and the fact that no other buckling mode preceded general instability. These other sources of test data[20-22] shown as Groups D, E, and F in Fig. 1 are summarized in Appendix 3. Summary plots of all the test data from all sources are also given in Appendix 3 together with a tabulation of pertinent orthotropic parameters.

The test data from all sources displayed in Fig. 1 were analyzed and then segregated as to their percent deviation from linear orthotropic theory. The synthesis of these data are shown in Fig. 2. It is quite clear from all the data that there is a singularity at the point (1, 1) representing isotropic cylinder behavior and the region of greatest deviation as well as scatter of test results. As one moves radially away from this point (with the possible exception of the third quadrant) the situation improves uniformly and acceptable agreement between linear orthotropic theory and experiment is obtained at the arbitrary distance indicated in Fig. 2.

An examination of buckle wavelengths in this enclosed region can provide some theoretical clues as to the apparent unusual sensitivity to imperfections. Eq. (1) indicates that for $\alpha=\gamma$, the 45 degree line in Fig. 2 represents a singularity for which the wavelength ratio β can theoretically assume any value between 0 and infinity. Also, beyond (1, 1), the axisymmetric mode governs as indicated in Fig. 1, so that our discussion is basically confined to the line segment $\overline{O1}+$.

It is also well known that a structure is sensitive only to small imperfections whose wavelengths correspond to those in which the structure would buckle if it were perfect. If we now hypothesize that a cylindrical shell structure contains some random distribution of small imperfection wavelengths, then it is quite apparent that in the

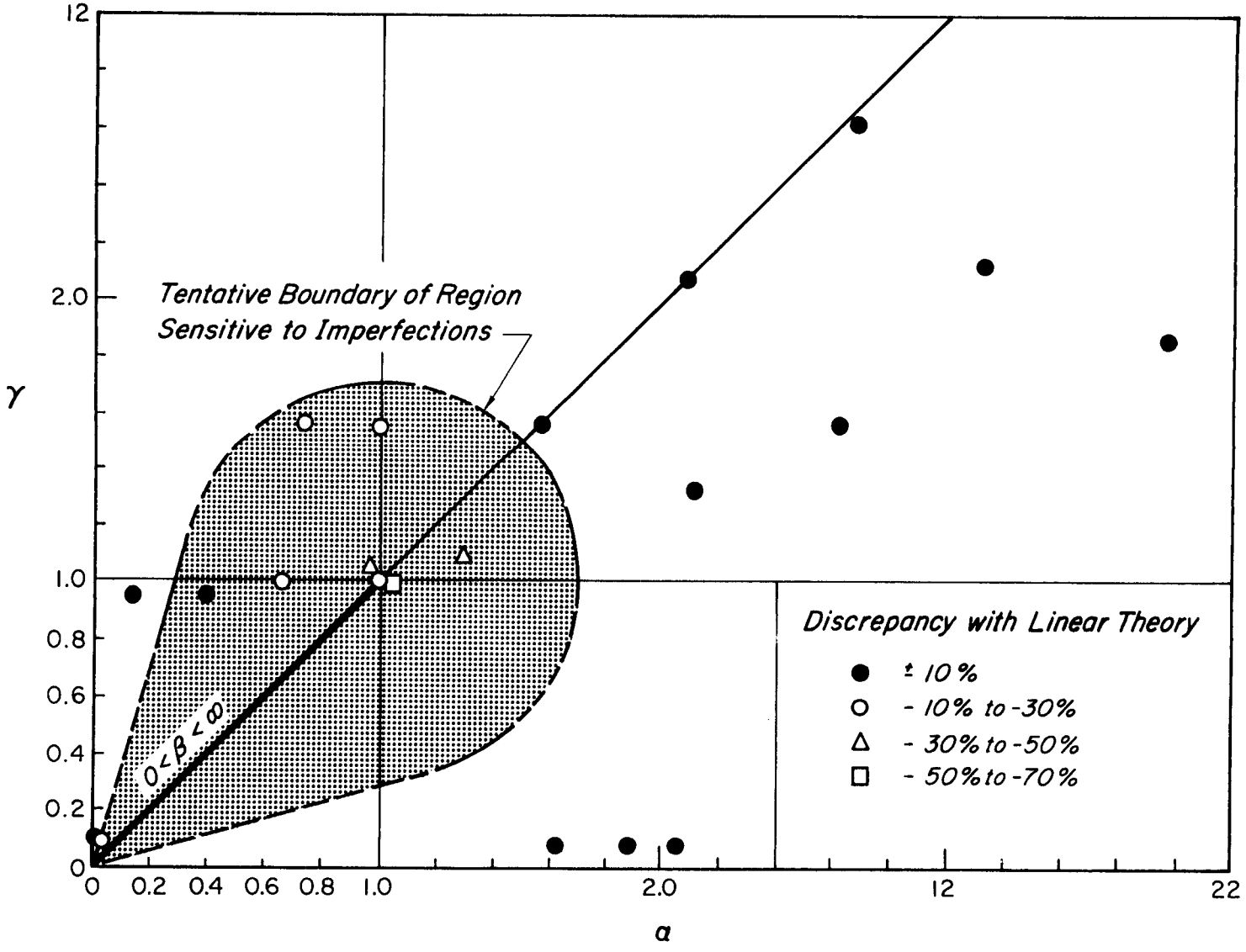

Figure 2 Synthesis of available test data on compressive stability of orthotropic cylinders under compression.

neighborhood of the line segment $\overline{OI}+$, any imperfection wavelength will buckle the shell into that form initially and prematurely. For the cylindrical shell under compression, the imperfection determines the initial buckle form because the perfect waveform is itself indeterminate. This situation which appears to be unique for a cylindrical shell under compression with orthotropic parameters corresponding to the line segment $\overline{OI}+$ is the reverse of that normally found for other types of structural elements and loadings. As one moves away from this critical line segment, β becomes determinate and the unusual sensitivity to imperfections begins to disappear. This trend is particularly evident for the longitudinally stiffened cylinder data of Groups A and D.

It is obviously highly desirable that further experimental data be obtained and analyzed to better define the region sensitive to initial imperfections. In the meantime, it is proposed to use the region defined in Fig. 2 on the basis of current test data for this purpose. It is believed that outside the cross hatched region linear orthotropic theory can be used with reasonable confidence to predict the general instability of compressed, symmetrically stiffened orthotropic cylinders. In the subsequent minimum weight analyses we shall return to Fig. 2 to be sure that results are obtained which will be outside of the initial imperfection region and which thus can achieve an acceptable degree of reliability consistent with minimum weight.

3. Minimum Weight Design Approach

Having established in Section 2 that there are indeed regions of orthotropic parameters where good agreement exists between linear general instability theory and test data on stiffened cylindrical shells, we turn now to our basic approach to the minimum weight design of such shells. In doing so, it is important to establish a basic physical picture of the behavior of minimum weight shells since there may be important differences in the interrelationship of the pertinent stability modes as the curvature of the cylindrical shell is varied. For this purpose now, we shall review minimum weight design aspects of a transversely supported wide column under compression and then proceed to generalize these results to a cylindrical shell.

Transversely Supported Flat Wide Column

The minimum weight analysis of transversely supported flat wide columns is contained in Ref. 23 for flexural types of ribs and in Ref. 24 for deflectional types. In either case, the essential results are the same and we shall extract here the essential physical features of the buckling modes and their relation to the minimum weight design of such structures. Fig. 3 indicates the general configuration of the structure assumed as well as other assumptions concerning boundary conditions, relative geometries and the idealization of the lateral stiffeners.

The behavior of the structural arrangement shown in Fig. 3 is fairly well understood and can be summarized as shown in Fig. 4. The main feature is the existence of a critical value of the spring constant parameter KL_t^3/D_1 which divides the regions of general instability (buckling over supports) and local instability (buckling between supports). Discrete element theory provides the correct transition between the two modes. Smeared element or orthotropic theory agree in the region indicated; orthotropic theory essentially ignores the existence of the local instability mode when extended beyond the region of agreement, unless the arbitrary cut-off indicated in Fig. 4 is utilized.

In conducting a minimum weight investigation of the configuration shown in Fig. 3 it is convenient to use the concept of solidity as a non-dimensional measure of weight. In terms of the parameters of Fig. 3,

$$\Sigma = t_s/h + A_r/hL_t \tag{6}$$

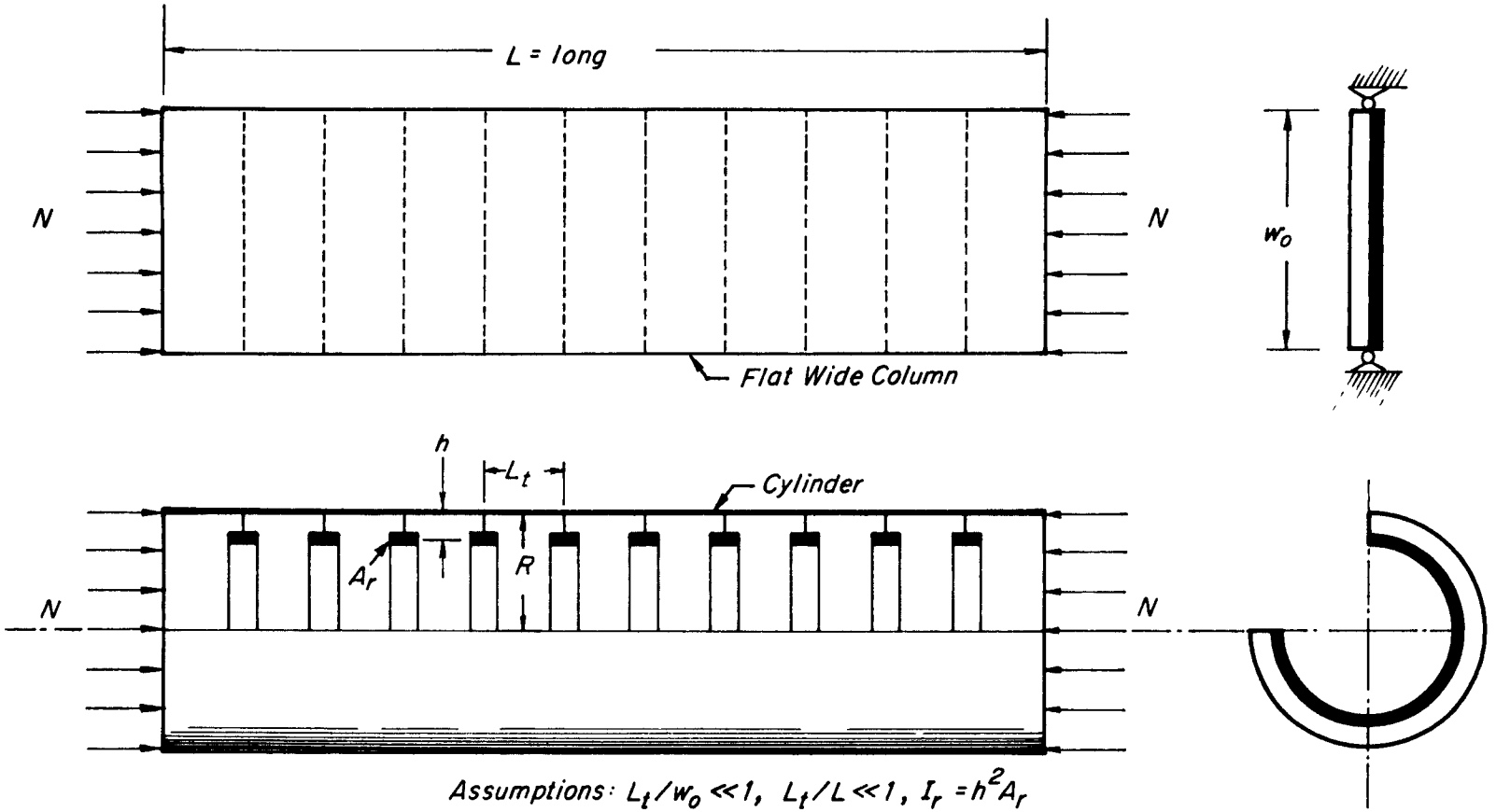

Figure 3 Geometry of idealized structural elements used in minimum weight analysis.

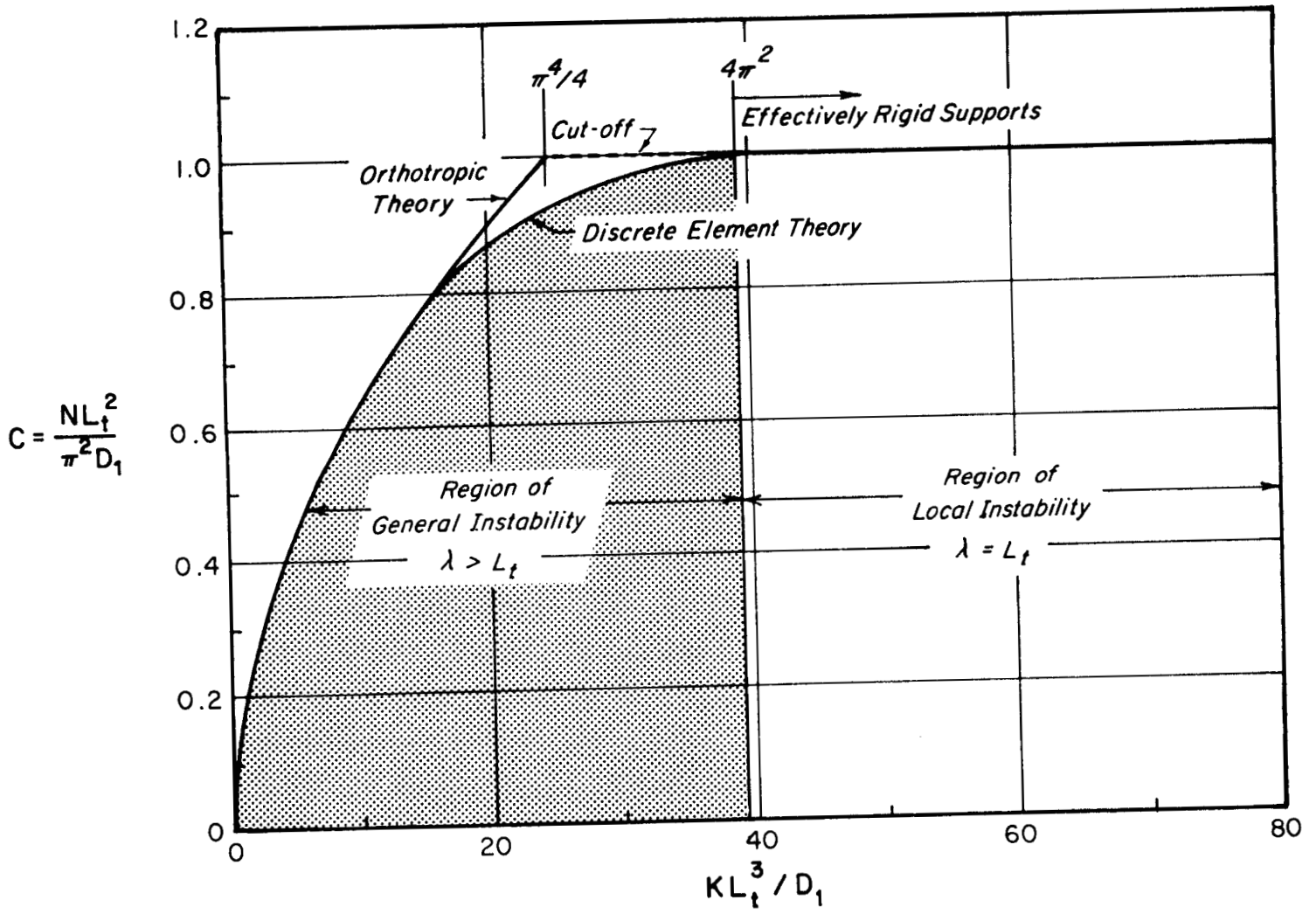

Figure 4 Buckling response of flat transversely supported wide columns.

The corresponding parameters presented in Fig. 4 are represented by

$$D_1 = Et_s^3/12(1-\nu^2)$$

$$K = \pi^4 E h^2 A_r / w_o^4 \qquad (7)$$

Typical results obtained by use of Fig. 4 and Eqs. (6) and (7) are displayed in Fig. 5 where relative solidity is shown as a function of the normalized stiffness parameter, $(KL_t^3/D_1)/4\pi^2$. Based upon discrete element theory, a minimum weight design is obtained at a point considerably below the critical value of KL_t^3/D_1 at which an effectively rigid supporting structure is first achieved. However, the solidity at the critical point where the general instability and local instability stresses are equal is only slightly higher than at the minimum. Also shown in Fig. 5 is the fact that orthotropic theory results in a minimum based upon the arbitrary cut-off shown in Fig. 4. Although this is a false minimum in a physical sense, it does provide a convenient and satisfactory approximation for the discrete element case.

Ring Supported Cylinder

Having reviewed the essential features of the flat panel, we turn now to the ring supported cylinder shown in Fig. 3 which in the limit becomes the flat panel. It is assumed that general instability of cylinders under compression occurs in the axisymmetric mode as would be expected from Fig. 1.

The introduction of curvature immediately introduces circumferential membrane stiffnesses as an important additional feature. For the cylinder, the skin contributes its membrane stiffness as a foundation modulus or smeared set of springs in parallel with the smeared or discrete deflectional spring system contributed by the ring area parameter A_r/hL_t. This is obviously different than the flat case where the skin contributed no support stiffness and the transverse supports contributed flexural stiffness only. Since the relative contribution of skin and supporting structure depends upon the curvature, R, we shall examine a relatively simple model in which the solidity is defined in the same manner for the flat panel and cylinder.

In order to simplify the analysis without compromising the results obtained, it is convenient to consider all spring systems as smeared in order that orthotropic theory can be used throughout. The results obtained from this analysis will indicate that the final conclusions are obtained in the region where orthotropic theory is indeed valid.

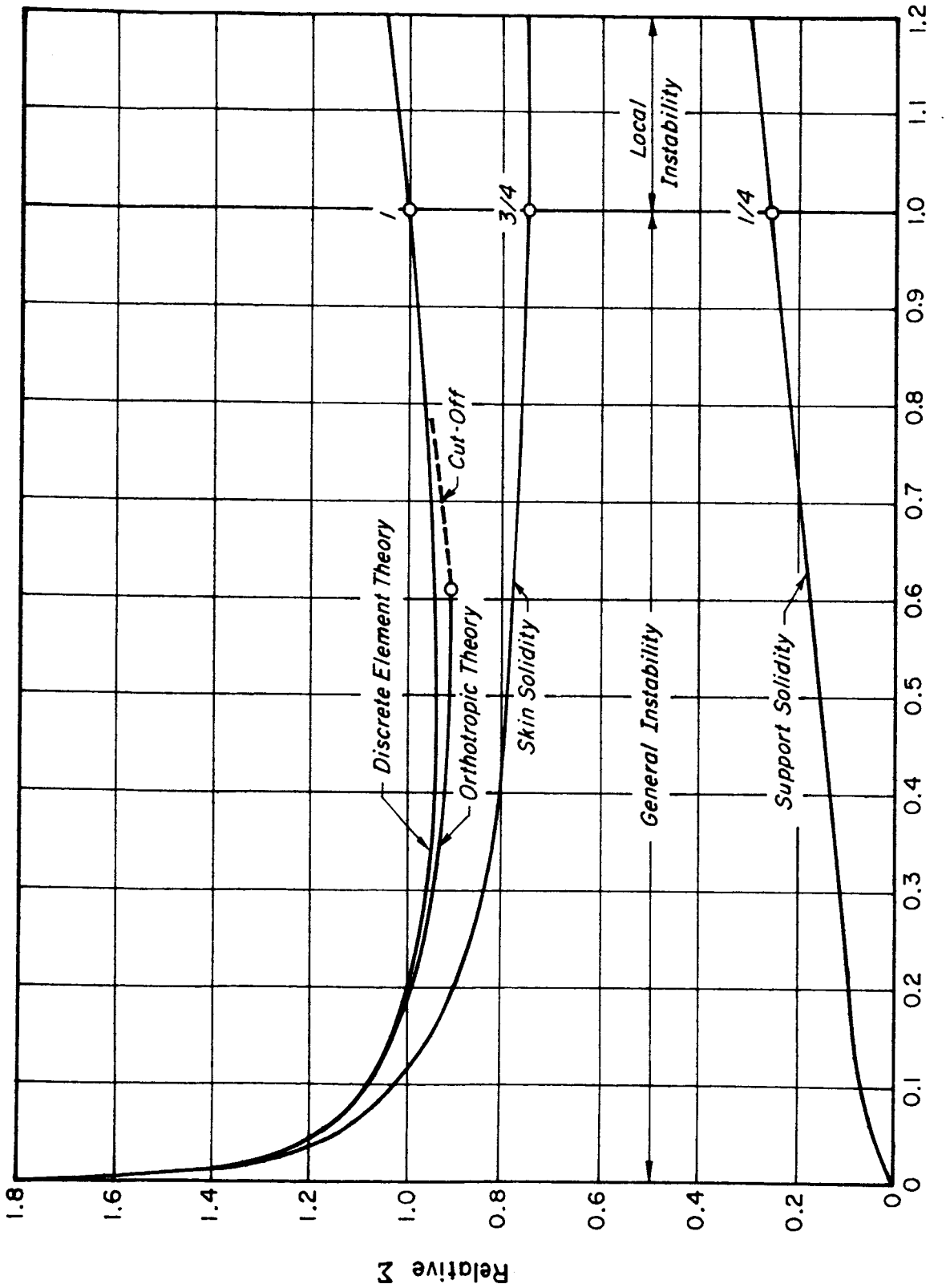

Figure 5 Relative solidity of flat transversely supported wide columns.

The governing equation for axisymmetric general instability of the ring supported cylinder shown in Fig. 3 is given by

$$D_1 \frac{\partial^4 w}{\partial x^4} + N \frac{\partial^2 w}{\partial x^2} + \left(\frac{B_2}{R^2} + \frac{K}{L_t}\right) w = 0 \tag{8}$$

where: $B_2 = E(t_s + A_r/L_t)/(1-\nu^2)$

and D_1 and K are defined in Eq. (7).

Assuming the following solution for Eq. (8), $w = a \sin(\pi x/\lambda)$, and minimizing the resulting expression with respect to λ, we obtain

$$N = 2\pi^2 D_1/\lambda^2 \tag{9}$$

and

$$(\lambda/\pi)^4 = (D_1 R^2/Eh)\left[\frac{t_s}{h} + \frac{A_r}{hL_t}\left(1 + \frac{\pi^4 h^2 R^2}{w_o^4}\right)\right]^{-1} \tag{10}$$

From Eqs. (9) and (10) and the definition of D_1 given by Eq. (7), we find that the required skin thickness t_s for a given loading N is given by

$$\left(\frac{t_s}{h}\right)^3 \left[\frac{A_r}{hL_t} + \left(\frac{t_s}{h} + \frac{A_r}{hL_t}\right)\frac{w_o^4}{\pi^4 h^2 R^2}\right] = \frac{3(1-\nu^2)}{\pi^2}\left(\frac{N}{Eh}\right)^2\left(\frac{w_o}{h}\right)^4 \tag{11}$$

Similarly, by eliminating D_1 in Eq. (10)

$$\bar{\lambda} = (2)^{1/2}\left[\left(\frac{N}{Eh}\right)^{1/2}\left(\frac{w_o}{h}\right)^2\right]^{-1}\pi \quad (\lambda/h) = \left[\frac{A_r}{hL_t} + \frac{1}{\pi^4}\left(\frac{t_s}{h} + \frac{A_r}{hL_t}\right)\left(\frac{w_o}{h}\right)^4\left(\frac{h}{R}\right)^2\right]^{-1/2} \tag{12}$$

For given values of (N/Eh) and (w_o/h) we can obtain from Eqs. (11) and (12) the variation of $\bar{\lambda}$ with the support area parameter A_r/hL_t for different values of R/h as shown in Fig. 6. It can be observed from Fig. 6 that when the panel is flat or only slightly curved, that there is a marked reduction in wavelength as the support area is increased. On the other hand, for $R/h < 100$ which is the region appropriate to practical stiffened cylinders, the wavelength is always finite and is

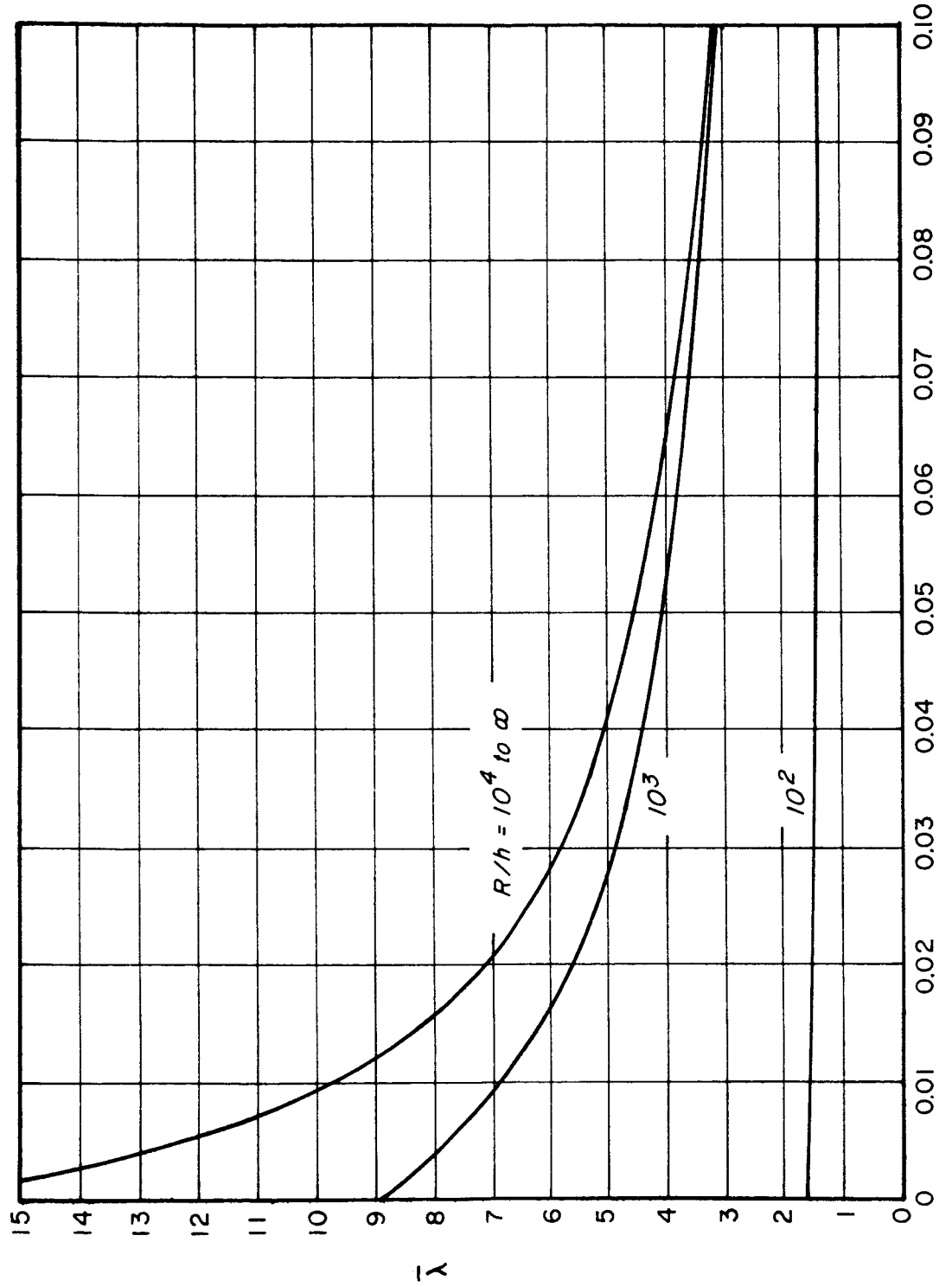

Figure 6 Wavelength parameter as a function of curvature for ring stiffened cylinders, ($N/Eh = 10^{-3}$, $w_o/h = 10$).

determined primarily by the skin membrane stiffness with little influence exerted by the supporting structure area.

We shall now consider the influence of this wavelength behavior upon the weight or solidity of the overall structure. For this purpose, we now define the solidity of the cylinder in the following special manner in order to be consistent with that for the flat panel

$$\Sigma = \frac{\bar{t} \times (\text{surface area})}{(\text{rib height}) \times (\text{surface area})} \tag{13}$$

Since $\bar{t}$ includes the skin plus smeared supporting structure area, Eq. (13) reduces to Eq. (6) for both cases.

From Eq. (11), we can obtain t_s/h as a function of A_r/hL_t for given values of N/Eh, and w_o/h. Fig. 7 plots Σ with respect to A_r/hL_t for various R/h values. It is interesting to note that for cylinders up to $R/h = 100$, the Σ curve rises with ring area and is the lowest for zero ring area indicating that the skin membrane stiffness is of primary importance. This is in contrast with flat plate behavior where a certain rib area provides for minimum weight, hence, an optimum design. For very high R/h values the influence of curvature is small, the skin stiffness plays a secondary role while the rib area is of primary importance in obtaining a minimum weight design.

The significance of curvature is thus demonstrated rather directly by the use of the orthotropic theory. We see that in the case of a flat plate the supporting system prevents buckling as a wide column and hence helps to raise the buckling stress. The weight of the supporting system is thus compensated by an increase in the buckling stress and a weight optimization can be achieved. For the cylinder of sufficient curvature, the skin assumes the role of the supporting system in the flat panel to prevent it from buckling as a column; the addition of rings adds to the weight without changing the buckling characteristics significantly.

Thus, in contrast to the flat case, minimum weight is not achieved upon simultaneous buckling in the general instability and local instability modes. If sufficient ring area is added to force this situation, a heavier design is always obtained than that corresponding to the perfect cylinder with zero ring area.

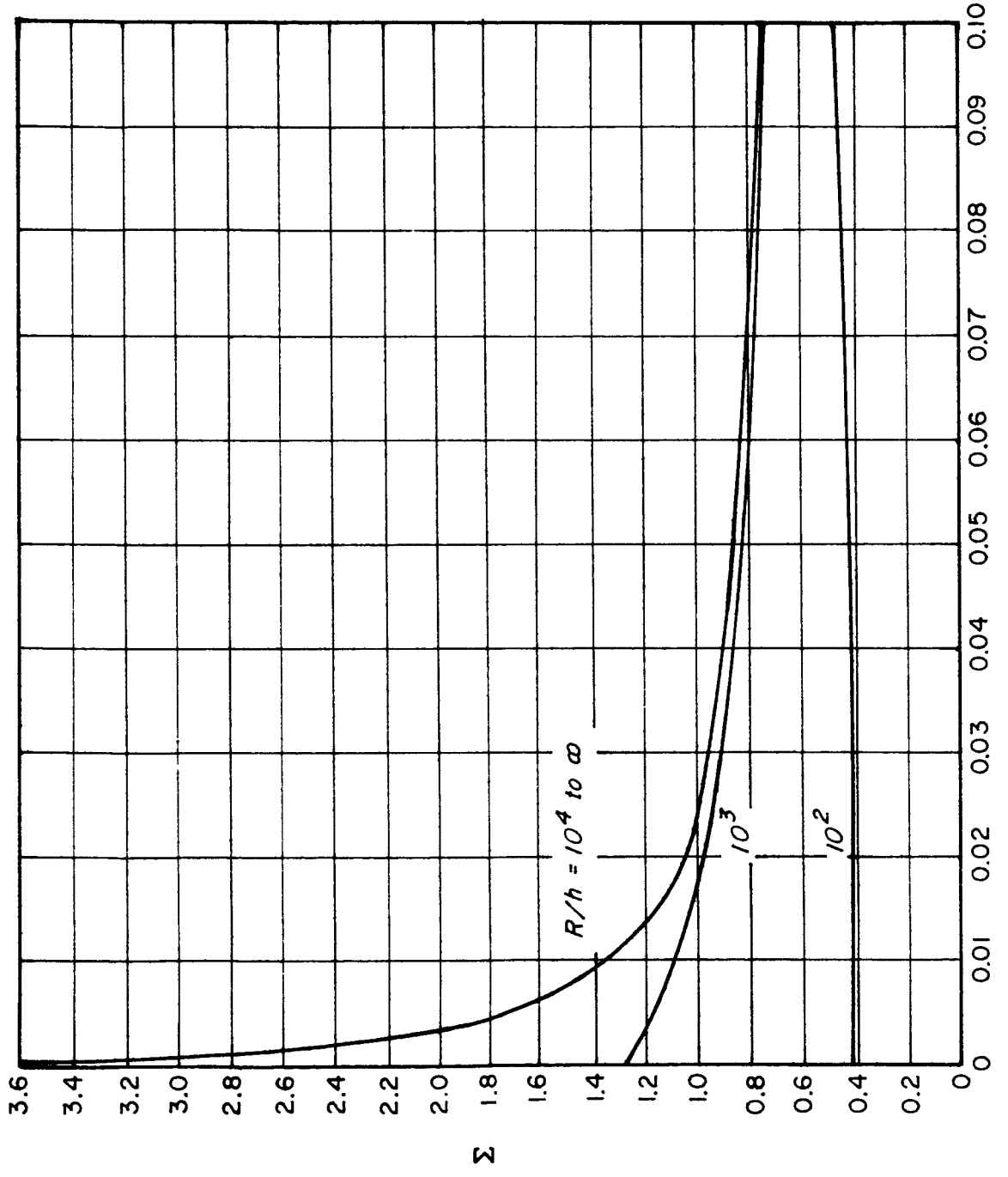

Figure 7 Solidity as a function of curvature for ring stiffened cylinders, ($N/Eh = 10^{-3}$, $w_o/h = 10$).

4. Minimum Weight Design of Orthotropic Cylinders Under Compression

The material contained in Sections 2 and 3 essentially provides a frame of reference and physical background for the assumptions to be utilized in the following minimum weight analysis. Because of the restrictions necessarily imposed upon the analysis in the interests of obtaining a relatively simple and direct solution, it should be recognized that while the results obtained represent minimum weight designs they may not constitute absolute minimums. Further research effort is warranted in this area when the details of the boundary shown in Fig. 2 are further clarified.

Because of the present uncertainites concerning the range of applicability of linear orthotropic theory, the minimum weight analysis is presented in sufficiently general form that changes in the boundary shown in Fig. 2 can be readily corrected for. Furthermore, although the analysis is conducted for compressive loading, it is apparent from the results presented in Appendix 2 that the analysis is equally valid for bending.

Assumptions

Orthotropic theory for symmetrical stiffening systems is employed herein in the interest of simplifying a rather complex problem. The effect of stiffener asymmetry for the geometric proportions associated with minimum weight designs is presently unknown. Thus, the results obtained herein for symmetrical systems can provide useful data for investigating the significance of asymmetry upon minimum weight designs.

As a result of the information developed in Section 3, it is assumed for this analysis that the stiffened cylindrical shells have sufficient curvature ($R/h < 100$) that the skin membrane stiffness dominates in establishing the general instability buckle weavlength. Under these circumstances, the wavelength (λ) will exceed the frame spacing (L_t) and there will be no condition imposed upon the minimum weight design that $\lambda = L_t$ as is usual for the flat panel. The appropriate value of λ or its equivalent function thus becomes the parameter that minimizes the weight.

The minimum weight analysis is conducted in a quite general form and includes the following cylindrical shell forms: perfect isotropic, ring stiffened, longitudinally and ring stiffened. For the first two cases, only the general instability buckling mode is involved. For the longitudinally stiffened case, the general instability mode corresponds to Euler buckling of the stiffened wide columns in the wavelength

λ. Since the stiffened wide columns used in this analysis are of optimum design, local instabilities of any of the stiffener elements will occur simultaneously at general instability.

For specified design conditions of a compressive loading (N) and buckle half wavelength (λ) corresponding to the simply supported length, the optimum stress of a wide column or a longitudinally stiffened wide column can be expressed in the following form.[23-25]

$$\sigma_o = \alpha_p E^{1-m} (N/\lambda)^m \tag{14}$$

In Eq. (14), the panel efficiency coefficient (α_p) represents the optimum geometric arrangement of stiffening elements in the cross section, and the exponent (m) depends upon the number of possible buckling modes. Both α_p and m have specific values for a given cross sectional shape.

Appropriate values of α_p and m obtained from Refs. 23-25 are presented in Table 1 for unstiffened wide columns as well as those with common Z and Y longitudinal stiffeners and improved Z and Y stiffeners recently developed in Ref. 25. In addition, the value of $(t_s/t_1)_o$ is given for subsequent use and represents the optimum skin thickness to smeared thickness in the longitudinal direction. In Fig. 8, the relative efficiencies of the various forms of stiffened wide columns are shown.

Table 1

Characteristics of Optimum Monolithic Wide Columns

Type		α_p	m	$(t_s/t_1)_o$
unstiffened		1.22	2/3	1.000
stiffened	- common Z	1.01	1/2	0.444
	- common Y	1.21	1/2	0.344
	- improved Z	0.984	4/9	0.305
	- improved Y	1.265	4/9	0.241

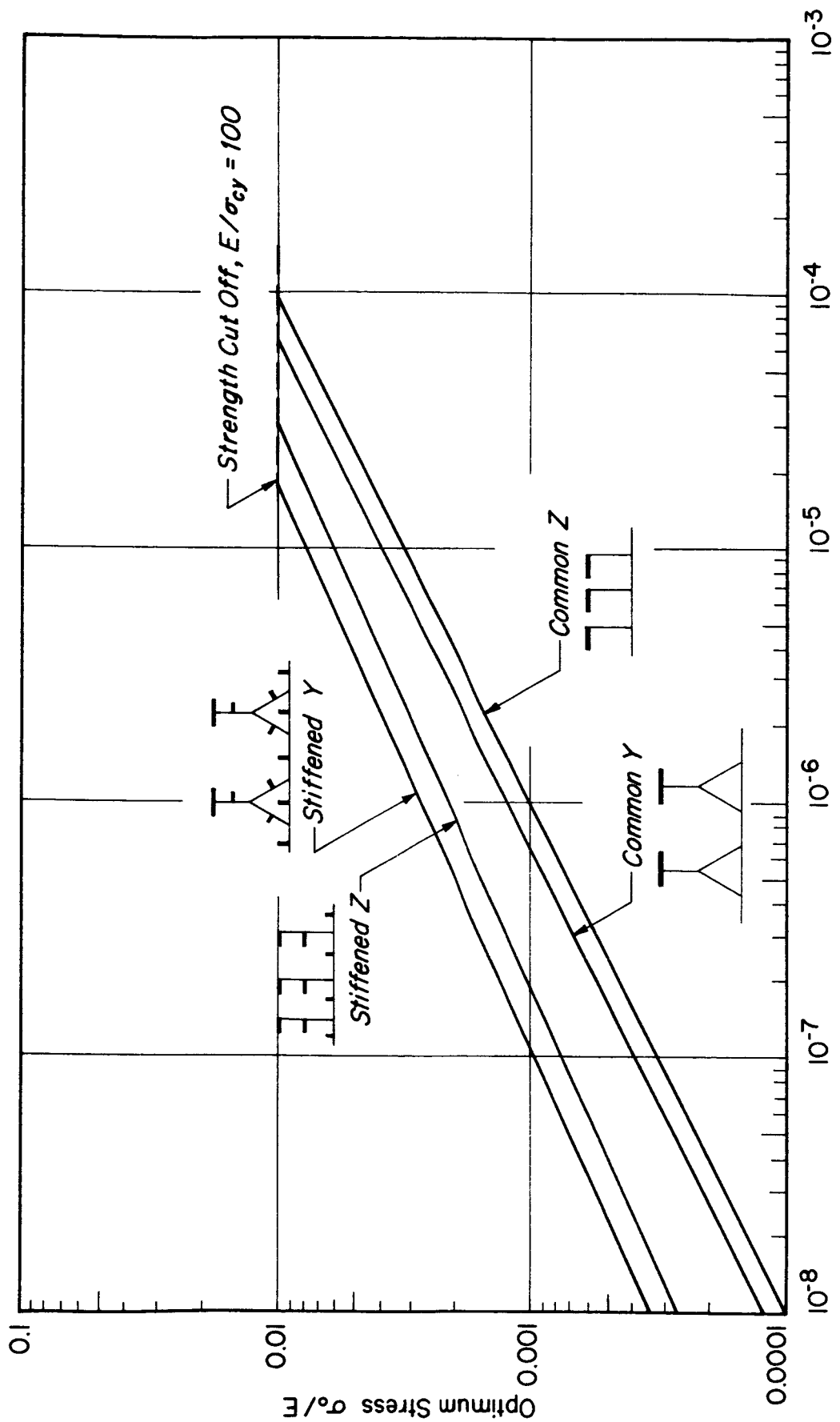

Figure 8 Comparative structural efficiencies of common and improved stiffened wide columns under compression.

Minimum Weight Analysis

In addition to the optimum wide column stress relation given by Eq. (14), we have available the compressive general instability stress relationship for orthotropic cylinders. Because of the data contained in Fig. 2, we shall restrict our analysis to the "safe" regions of Zones III to VI which encompasses the axisymmetric and asymmetric m-continuous modes but excludes the asymmetric m=1 mode. As shown in Appendix 2, the buckling load for the two modes to be considered can be written in the following form from Eq. (2).

$$N = (4/d)(1-\nu^2)^{1/2}(B_2D_1)^{1/2}U \tag{15}$$

For the axisymmetric case U=1 while for the asymmetric case U<1. Hence, in general, $U \leq 1$.

In both Eq. (14) and (15), the loading (N) is related to the applied stress (σ_a) through the usual relation

$$\sigma_a = N/t_1 \tag{16}$$

In Eqs. (15) and (16), the subscripts 1, 2 refer to the axial and circumferential directions, respectively. Furthermore, it is convenient to define the following geometrical parameters

$$k_a = B_2/B_1 \qquad \alpha k_a = D_2/D_1 \tag{17}$$

The solidity of the cylindrical shell is now defined in the usual manner as the volume of structural material relative to the enclosed volume. For a cylinder of diameter (d)

$$\Sigma = 4\,(t_1/d + A_r/L_t d) \tag{18}$$

However,

$$\frac{A_r}{L_t d} = \frac{t_2 - t_s}{d} = \frac{t_1}{d}\,(k_a - t_s/t_1) \tag{19}$$

Substituting Eq. (19) into (18)

$$\frac{\Sigma}{4} = \frac{t_1}{d}\,(1 + k_a - t_s/t_1) \tag{20}$$

For an optimum wide column, (t_s/t_1) is fixed as indicated in Table 1. If k_a is treated as a parameter that minimizes the solidity, then the essential step at this point is to replace the quantity (t_1/d) by the loading (N) and diameter (d) which are the specified quantities for the design problem.

By use of Eqs. (14) and (16), we can immediately obtain

$$\frac{t_1}{d} = \frac{1}{\alpha_p}\left(\frac{N}{Ed}\right)^{1-m}\left(\frac{\lambda}{d}\right)^{m} \tag{21}$$

The wavelength λ is, of course, unknown at this point and it is necessary to utilize the general instability relation, Eq. (15) and its associated λ expression to solve Eq. (21). From Appendix 2, the following convenient expression has been developed, Eq. (B. 21)

$$\lambda = (2\pi^2 U^2 X^2 D_1/N)^{1/2} \tag{22}$$

where X is a function of $\overline{\beta}$. For our purposes here, it is sufficient that we know that $X \geq 1$ for the asymmetric m-continuous mode and $X = 1$ for the axisymmetric mode.

We now turn to Eq. (15) and by substituting $B_2 = k_a E t_1/(1-\nu^2)$ as defined by Eq. (17), and the relation given by Eq. (22) for D_1, we obtain

$$\frac{t_1}{d} = \frac{\pi^2}{8}\,\frac{X^2}{k_a}\left(\frac{N}{Ed}\right)\left(\frac{d}{\lambda}\right)^2 \tag{23}$$

By equating Eqs. (21) and (23)

$$\left(\frac{\lambda}{d}\right)^{2+m} = \frac{\pi^2}{8}\,\frac{X^2}{k_a}\,\alpha_p\left(\frac{N}{Ed}\right)^{m} \tag{24}$$

By utilizing Eq. (24) in (23) or (21) to eliminate λ/d

$$\frac{t_1}{d} = \left(\frac{\pi^2 X^2}{8k_a}\right)^{m/2+m}\left(\frac{1}{\alpha_p}\right)^{2/2+m}\left(\frac{N}{Ed}\right)^{(2-m)/2+m} \tag{25}$$

Finally, by substituting Eq. (25) for t_1/d in Eq. (20), the following general expression is obtained for the solidity

$$\frac{\Sigma}{4} = \left(\frac{\pi^2 X^2}{8}\right)^{m/2+m}\left(\frac{1}{\alpha_p}\right)^{2/2+m}\left(\frac{N}{Ed}\right)^{(2-m)/2+m}\left\{\left(1-\frac{t_s}{t_1}\right)(k_a)^{-m/2+m} + (k_a)^{2/2+m}\right\} \tag{26}$$

In the following, we will discuss results for various specific types of stiffening systems whose characteristics are given in Table 1.

It is quite evident that for a given stiffener of optimum design, α_p, m and t_s/t_1 are fixed and the loading parameter N/Ed is prescribed. Thus, the two remaining factors in Eq. (26) are k_a which we shall consider in the following and the parameter X where for the axisymmetric mode X = 1 and for the asymmetric m-cont. mode $X \geq 1$. From the characteristics of X it is evident that buckling in the axisymmetric mode will always result in a solidity less than or equal to that corresponding to the asymmetric m-cont. case. Thus, minimum weight designs should conform to Zones V and VI of Fig. 1.

Minimum Weight Results - Isotropic Cylinders

Having established the general solidity relation for orthotropic cylinders, we can now proceed to obtain specific results. The first case to be considered is the perfect isotropic cylinder of moderate length. Here the axisymmetric and asymmetric modes are equal, X = 1, and by definition for an isotropic cylinder, $k_a = t_s/t_1 = 1$. Furthermore, from Table 1 for an unstiffened wide column, m = 2/3 and $\alpha_p = 1.22$. Thus, Eq. (26) reduces to the following for this case

$$\Sigma = 3.63\,(N/Ed)^{1/2} \tag{27}$$

The analysis of cylindrical shells containing imperfections has been presented previously in Ref. 26. In terms of the solidity defined herein

$$\Sigma = 1.40\,(N/Ed)^{2/5} \tag{28}$$

Results also have been obtained previously for honeycomb sandwich cylinders which constitute another form of isotropic shell. For a sandwich with face density to core density of 50, the following optimum solidity is obtained from Ref. 27

$$\Sigma = 1.02\,(N/Ed)^{1/2} \tag{29}$$

Eqs. (28) and (29) will provide useful references in the subsequent comparative efficiency analysis.

Minimum Weight Results - Stiffened Cylinders

The simplest form of stiffened cylinder consists of the addition of rings or frames to an isotropic skin. Such cylinders will always buckle in the axisymmetric mode and therefore $X = 1$. Furthermore, with $m = 2/3$, $\alpha_p = 1.22$ and $t_s/t_1 = 1$ for this case from Table 1, Eq. (26) reduces to

$$\Sigma = 3.63\,(k_a)^{3/4}\,(N/Ed)^{1/2} \tag{30}$$

Since $k_a > 1$ for this case, it is apparent that the addition of rings only serves to decrease the efficiency of a perfect cylinder, Eq. (27). The situation is somewhat different when imperfect cylinders which behave according to Eq. (28) are considered.

If we replace the isotropic skin of the previous example with an optimum longitudinally stiffened skin and furthermore restrict the design to the efficient axisymmetric Zones V and VI, then $X = 1$ in Eq. (26). For a given optimum panel design which fixes α_p, m and t_s/t_1, it would appear that an optimum value of k_a can be established by performing the operation $\partial\Sigma/\partial k_a = 0$ on Eq. (26).

$$(k_a)_o = (1-t_s/t_1)\,m/2 \tag{31}$$

Since $k_a \geq t_s/t_1$, Eq. (31) generally results in a false optimum for the values given in Table 1 and the cut-off condition $k_a \geq t_s/t_1$ must be used instead.

In general, Eq. (26) can be replaced by

$$\Sigma = C(N/Ed)^n \tag{32}$$

where C is a function of m, α_p, t_s/t_1 and the value chosen for k_a. Appropriate values of n and C for $k_a = t_s/t_1$ which implies zero ring area or longitudinally stiffening only are given in Table 2 together with a summary of such values for the other cases.

Unfortunately, the results obtained when $k_a = t_s/t_1$ or zero ring area necessarily place these designs in the region of $\alpha < 1$ and $\gamma > 1$ in Fig. 2. The latter condition results from our assumption of axisymmetric buckling, $X = 1$. Such designs are potentially unreliable since they probably fall in the shaded zone of Fig. 2. Since we desire to restrict the minimum weight analysis to those regions where linear orthotropic stability is valid, we must now consider the addition of sufficient ring area to the longitudinally stiffened cylinder to achieve axisymmetric buckling in Zones V and VI.

From Fig. 2, it would appear that a satisfactory criterion to achieve axisymmetric buckling would be to require that $\alpha \geq 1.8$. For this purpose, it is convenient to assume that $k_a = 1$ and by virtue of Eq. (17), then $D_2/D_1 \geq 1.8$. The latter can generally be satisfied through use of the ring stiffening configuration shown in Fig. 3 since there is no particular restriction on h for the rings. By letting $k_a = 1$ in Eq. (26), the C values given in Table 2 for ring stiffened cylinders were obtained in conjunction with the specific values given in Table 1. It can be observed that there is some weight penalty as compared to the longitudinally stiffening only case. A summary plot of the data contained in Table 2 is presented in Fig. 9. For the longitudinally stiffened cylinders, only the $k_a = 1$ results are shown, to conform to the spirit of this analysis.

Table 2

Characteristics of Optimum Orthotropic Cylinders

Type	n	C
a. isotropic		
perfect	1/2	3.63
imperfect	2/5	1.40
sandwich	1/2	1.02
b. longitudinally stiffened		
common Z	3/5	4.91*
common Y	3/5	4.44*
improved Z	7/11	5.22*
improved Y	7/11	4.45*
c. ring stiffened		
isotropic skin	1/2	$3.63\,(k_a)^{3/4}$
common Z	3/5	6.48**
common Y	3/5	5.93**
improved Z	7/11	7.14**
improved Y	7/11	6.01**

* corresponds to zero ring area, $k_a = t_s/t_1$

**corresponds to $k_a = 1$

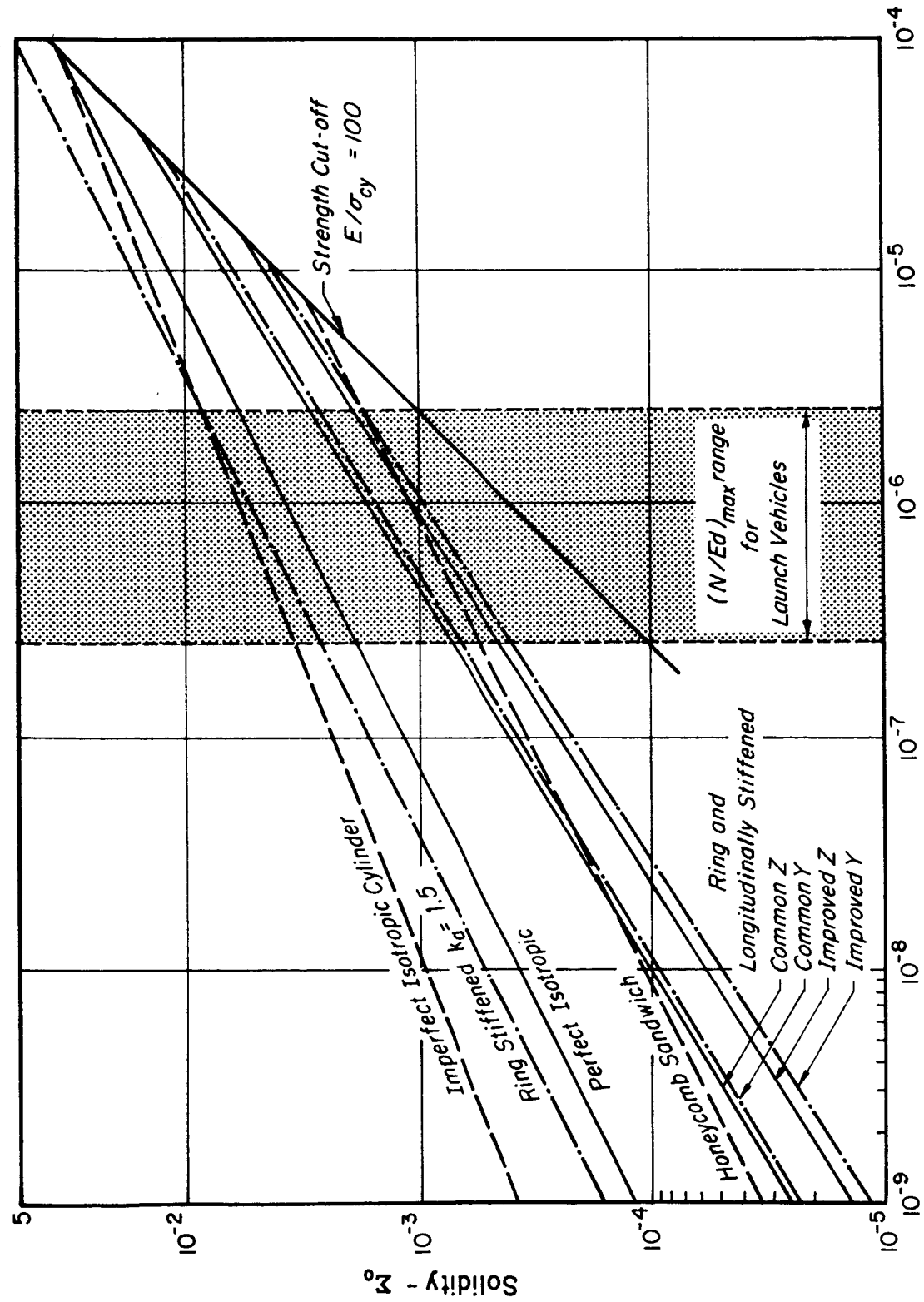

Figure 9 Comparative structural efficiencies of various types of stiffened cylinders under compression.

5. Conclusions

Within the restrictions imposed upon the minimum weight analysis that the designs must conform to those regions where linear orthotropic stability theory and available experimental data are in good agreement, the results obtained herein and summarized in Fig. 9 are reviewed to establish their significance. The following conclusions appear to emerge from the analysis:

1. As compared to a perfect isotropic cylinder, the use of ring stiffening alone results in a decrease in efficiency. Practically, however, ring stiffening tends to make an imperfect isotropic cylinder behave as a perfect cylinder by suppressing its sensitivity to imperfections. In this respect, ring stiffening can result in a substantial improvement in efficiency particularly at lower values of the loading index.

2. In direct contrast with (1) above, combinations of ring and longitudinal stiffeners can result in significant improvements in efficiency as compared to perfect isotropic cylinders.

3. For the launch vehicle maximum (N/Ed) range, common stiffening shapes are not directly competitive with perfect honeycomb sandwich cylinders. At lower values of N/Ed, the situation becomes considerably more competitive. Furthermore, the improved stiffener shapes are competitive or superior to honeycomb sandwich as well as offering significant weight saving potential as compared to the common shapes.

4. Because of the similarity in behavior of perfect honeycomb sandwich cylinders and perfect isotropic cylinders, use of rings only on the sandwich cylinder cannot improve its efficiency. Rings conceivably could improve the performance of imperfect sandwich cylinders.

References

1. Gerard, G., "Optimum Structural Design Concepts for Aerospace Vehicles," J. Spacecraft and Rockets, Vol. 3, No. 1, pp. 5-18, Jan. 1966.

2. Flügge, W., "Die Stabilität der Kreiszylinderschale," Ing. - Archiv, Vol. 3, No. 5, pp. 463-506, Dec. 1932.

3. Dschou, D., "Die Druckfestigkeit Versteifter Zylindrischer Schalen," Luftfahrtforschung, Vol. 11, No. 8, pp. 233-234, Feb. 1935.

4. Taylor, J. L., "The Stability of a Monocoque in Compression," A.R.C., R and M 1679, 1935.

5. Anon., "Some Investigations of the General Instability of Stiffened Metals Cylinders. I - Review of Theory and Bibliography," NACA TN 905, 1943.

6. Becker, H., "Handbook of Structural Stability, Part VI - Strength of Stiffened Curved Plates and Shells," NACA TN 3786, July 1958.

7. Becker, H., "General Instability of Stiffened Cylinders," NACA TN 4237, 1958.

8. Becker, H., and Gerard, G., "Elastic Stability of Orthotropic Shells," J. Aerospace Sci., Vol. 29, No. 5, pp. 505-513, May 1962.

9. Thielemann, W. F., "New Developments in the Nonlinear Theories of the Buckling of Thin Cylindrical Shells," Aeronautics and Astronautics, Pergamon Press, London, 1960, pp. 76-119.

10. Gerard, G., "Plastic Stability Theory of Geometrically Orthotropic Plates and Cylindrical Shells," J. Aerospace Sci., Vol. 29, No. 8, pp. 956-962, Aug. 1962.

11. Gerard, G., "Compressive Stability of Orthotropic Cylinders," J. Aerospace Sci., Vol. 29, No. 10, pp. 1171-1180, October 1962.

12. Almroth, B. O., "Postbuckling Behavior of Orthotropic Cylinders Under Axial Compression," AIAA Journal, Vol. 2, No. 10, pp. 1795-1799, Oct. 1964.

13. DeLuzio, Stuhlman, G. E. and Almroth, B. O., "Influence of Stiffener Eccentricity and End Moment on the Stability of Cylinders in Compression," AIAA 6th Structures and Materials Conference, AIAA, New York, N.Y., 1965, pp. 117-124.

14. Block, D. L., Card, M. F., Mikulas, M. M., "Buckling of Eccentrically Stiffened Orthotropic Cylinders," NASA TN D-2960, Aug. 1965.

15. Milligan, R. W., Gerard, G., Lakshmikantham, C., "General Instability of Orthotropically Stiffened Cylinders Under Axial Compression," AIAA Preprint No. 66-139, Jan. 1966.

16. Milligan, R., Gerard, G., Lakshmikantham, C., and Becker, H., "General Instability of Orthotropically Stiffened Cylinders. Part I - Axial Compression, Torsion and Hydrostatic Pressure Loadings," Air Force Flight Dynamics Laboratory, Tech. Rept. AFFDL-TR-65-161, Pt. I, July 1965.

17. Lakshmikantham, C., Gerard, G., and Milligan, R., "General Instability of Orthotropically Stiffened Cylinders. Part II - Bending and Combined Compression and Bending," Air Force Flight Dynamics Laboratory, Tech. Rept. AFFDL-TR-65-161, Pt. II, Aug. 1965.

18. Becker, H., Gerard, G., and Winter, R., "Experiments on Axial Compressive General Instability of Monolithic Ring-Stiffened Cylinders," AIAA J., Vol. 1, No. 7, pp. 1614-1618, July 1963.

19. Tasi, J., Feldman, A., and Stang, D. A., "The Buckling Strength of Filament-Wound Cylinders Under Axial Compression," NASA CR-266, July 1965.

20. Katz, L., "Compression Tests on Integrally Stiffened Cylinders," NASA TM X-53315, August 1965.

21. Peterson, P., and Anderson, K., "Test of a Truss-Core Sandwich Cylinder Loaded to Failure in Bending," NASA TN D-3157, Dec. 1965.

22. Peterson, J. P., and Anderson, J. K., "Structural Behavior and Buckling Strength of Honeycomb Sandwich Cylinders Subjected to Bending," NASA TN D-2926, August 1965.

23. Gerard, G., Minimum Weight Analysis of Compression Structures, New York University Press, New York, 1956, pp. 50-63.

24. Gerard, G., Introduction to Structural Stability Theory, McGraw-Hill Book Co., New York, 1962, pp. 89-103.

25. Papirno, R., and Gerard, G., "Longitudinally Stiffened Wide Columns of Improved Efficiency," Allied Research Associates, Inc., Tech. Rept. ARA 292-1, Sept. 1965.

26. Gerard, G., "An Evaluation of Structural Sheet Materials in Missile Applications," Jet Propulsion, Vol. 28, No. 8, pp. 511-520, August 1958.

27. Williams, M. L., Gerard, G., and Hoffman, G. A., "Selected Areas of Structural Research in Rocket Vehicles," XI International Astronautical Congress, Stockholm, Vol. 1, pp. 146-166, 1960.

Additional Symbols for Appendices 1 and 2

A_{ij}	plasticity coefficients
b_i	stiffener spacing
$\bar{E}$	generalized elastic modulus
E_s	secant modulus
E_t	tangent modulus
I_i	moment of inertia
M	bending moment per unit width
$[m_i]$	3 x 3 submatrix
N	integer
p	pressure
u, v, w	displacements
α	plasticity factor
β^*	wavelength parameter for bending
ϵ_e	effective strain
μ_{ij}	membrane Poisson's ratio
ν_{ij}	flexural Poisson's ratio
$\bar{\nu}$	generalized Poisson's ratio
σ_e	effective stress
χ_{ij}	curvatures

Subscripts

x, y, θ	coordinates
b	bending
c	compression

Appendix 1

A General Linear Orthotropic Theory for Stability of Thin Shells

Introduction

Our objective here is to present a systematic development of a general elastic and plastic linear theory for the stability of orthotropic shells. The equilibrium and the kinematic equations which govern the shell stability are formulated in the simplest possible terms in the spirit of Donnell's assumptions for shallow curved panels. The constitutive equations include the orthotropic, elastic and plastic effects. The following development is based on Ref. 10.

Equilibrium Equations

A generic point on middle surface of the thin shell is described by an orthogonal curvilinear coordinate system (x, y) which follows the lines of curvature of the surface at the point. It is further assumed that the principal radii of curvature R_x, R_y at the point are different but constant. If N_x, N_y, N_{xy} represent a system of external loads per unit width, then the equilibrium of internal stress state with these constant external loads during the buckling process is satisfied by the following equations:

$$\partial N_x'/\partial x + \partial N_{xy}'/\partial y = 0$$

$$\partial N_{xy}'/\partial x + \partial N_y'/\partial y = 0$$

$$-[\partial^2 M_x'/\partial x^2 + 2\partial^2 M_{xy}'/\partial x \partial y + \partial^2 M_y'/\partial y^2] + N_x'/R_x + N_y'/R_y \qquad \text{(A. 1)}$$

$$+ N_x(\partial^2 w/\partial x^2) + 2N_{xy}(\partial^2 w/\partial x \partial y) + N_y(\partial^2 w/\partial y^2) + p = 0$$

In Eqs. (A.1), N_i' and M_i' represent the internal stress state produced during the buckling process, or more precisely, the variation in the initial stress state at buckling. In deriving the equilibrium equations (A.1), it is assumed that the shell expands freely to its prebuckled shape.

Kinematic Relations

The kinematic relations connecting the middle surface direct strains ϵ_1, ϵ_2, ϵ_3, and the curvature changes χ_1, χ_2, χ_3, with the displacement components u, v, and w are:

$$\begin{aligned} \epsilon_1 &= \partial u/\partial x + w/R_x & \chi_1 &= \partial^2 w/\partial x^2 \\ \epsilon_2 &= \partial v/\partial y + w/R_y & \chi_2 &= \partial^2 w/\partial y^2 \\ \epsilon_3 &= 1/2[\partial u/\partial y + \partial v/\partial x] & \chi_3 &= \partial^2 w/\partial x \partial y \end{aligned} \qquad (A.2)$$

Constitutive Laws

Since the plasticity effects for the stability problem are based on a deformation or total plasticity theory, which implies a unique relationship between an effective stress and an effective strain, we may write the elastic and plastic laws for a plane stress system applicable for thin shell studies, in the following manner:

$$\sigma_x = \frac{\bar{E}}{(1-\bar{\nu}^2)} [\epsilon_x + \bar{\nu}\epsilon_y]$$

$$\sigma_y = \frac{\bar{E}}{(1-\bar{\nu}^2)} [\epsilon_x + \bar{\nu}\epsilon_y] \qquad (A.3)$$

$$\sigma_{xy} = \frac{\bar{E}}{1+\bar{\nu}} \quad \epsilon_{xy} = \frac{\bar{E}}{(1-\bar{\nu}^2)} (1-\bar{\nu})\epsilon_{xy}$$

In Eqs. (A.3), if the shell is elastic $\bar{E} = E$, the Young's modulus and $\bar{\nu} = \nu$ the elastic Poisson ratio; if the shell is plastic, $\bar{\nu} \equiv 1/2$ and $\bar{E} = E_s$ the secant modulus given by

$$E_s = \frac{\sigma_e}{\epsilon_e}$$

with

$$\sigma_e = [\sigma_x^2 + \sigma_y^2 - \sigma_x\sigma_y + 3\sigma_{xy}^2]^{1/2} \qquad (A.4)$$

and

$$\epsilon_e = \frac{2}{\sqrt{3}} [\epsilon_x + \epsilon_y + \epsilon_x\epsilon_y + \epsilon_{xy}^2]^{1/2}$$

We can now write the relationship between the middle surface strain components ϵ_i, χ_i and the stress resultants N_i', M_i', using the fact that N_i', M_i', are related to σ_i through

$$N_i' = \int \sigma_i \, dz \qquad\qquad M_i' = \int \sigma_i \, z dz \qquad\qquad (A.5)$$

where z is the normal coordinate to the x, y surface and the integration is carried through the thickness of the shell. Then the stress resultants and the strain components are related through the following:

$$\begin{vmatrix} N_x'/B_1 \\ N_y'/B_2 \\ N_{xy}'/B_3 \\ M_x'/D_1 \\ M_y'/D_2 \\ M_{xy}'/D_3 \end{vmatrix} = \left|\begin{array}{c:c} & \\ [m_1] & [m_3] \\ & \\ \hdashline & \\ [m_4] & [m_2] \\ & \end{array}\right| \begin{vmatrix} \epsilon_x \\ \epsilon_y \\ \epsilon_{xy} \\ \chi_x \\ \chi_y \\ \chi_{xy} \end{vmatrix} \qquad (A.6)$$

In Eq. (A.6), each $[m_i]$ is a 3 x 3 sub-matrix. The sub-matrices $[m_3]$ and $[m_4]$ show the coupling between the membrane and bending terms and are of importance when the stiffening system is asymmetric. In general, bending about one axis will produce a membrane resultant about an orthogonal axis. The importance of the coupling depends upon the loading system and cross sectional geometry. Very seldom is it required to have a full 3 x 3 matrix for $[m_3]$ or $[m_4]$. Depending upon an analysis of the physical behavior and the geometry, only one term may be significant; as for example, in deep stiffeners it may be the height of the c. g. of the stiffener from the shell skin. In symmetric stiffening systems, $[m_3] = [m_4] = 0$.

The submatrices $[m_1]$ and $[m_2]$ together with rigidity terms B_i and D_i reflect the generalization of the stress-strain relations, Eq. (A.6), to include orthotropic effects. In the discussion of $[m_1]$ and $[m_2]$ it is convenient to differentiate between the orthotropic and isotropic cases.

Elastic Isotropic Case: For an elastic isotropic curved plate element symmetry demands that $[m_3] = [m_4] = 0$. Furthermore, $[m_1] = -[m_2]$; and $[m_1]$ is given by:

$$[m_1] = \begin{vmatrix} 1 & \nu & 0 \\ \nu & 1 & 0 \\ 0 & 0 & (1-\nu) \end{vmatrix} \qquad (A.7)$$

The rigidity terms are given by:

$$B_i = \frac{Et}{(1-\nu^2)} \qquad D_i = \frac{Et^3}{12(1-\nu^2)}$$

Elastic Orthotropic Case: An elastic orthotropic plate element possesses two axes of elastic symmetry in the plane of the plate and these coincide with the coordinate axes.

If the stiffening system for the plate is symmetric then $[m_3] = [m_4] = 0$. As for $[m_1]$ and $[m_2]$ however, we recognize that, since there are two axes of elastic symmetry, Poisson's ratio can be different in each direction. Furthermore, the Poisson ratio for membrane behavior is generally different from that of flexure. Hence, in general, $[m_1] \neq -[m_2]$ and each is given by

$$[m_1] = \begin{vmatrix} 1 & \mu_{12} & 0 \\ \mu_{21} & 1 & 0 \\ 0 & 0 & (1-\mu_{33}) \end{vmatrix} \qquad (A.8)$$

$$[m_2] = \begin{vmatrix} 1 & \nu_{12} & 0 \\ \nu_{21} & 1 & 0 \\ 0 & 0 & (1-\nu_{33}) \end{vmatrix} \qquad (A.9)$$

In Eqs. (A.8) and (A.9), the μ_{ij}, ν_{ij} terms refer to the Poisson ratios for the membrane and flexural cases, respectively, and the corresponding rigidities are given by:

$$\begin{aligned} B_1 &= Et_1/(1-\mu_{12}\mu_{21}) & D_1 &= EI_1/b_1(1-\nu_{12}\nu_{21}) \\ B_2 &= Et_2/(1-\mu_{12}\mu_{21}) & D_2 &= EI_2/b_2(1-\nu_{12}\nu_{21}) \\ B_3 &= Et_3/(1-\mu_{33}^2) & D_3 &= EI_3/b_3(1-\nu_{33}^2) \end{aligned} \qquad (A.10)$$

Thus, it becomes clear that in the case of an elastic orthotropic plate there are seven elastic constants to deal with, namely the six Poisson ratios and E the Young's modulus. Only experimental evidence can determine how markedly the Poisson ratio variation is in each direction and how much it influences the prediction of the results. Taylor[4], and Gerard and Becker,[6, 7, 8] have shown that in most of the problems of stiffened cylinders it is not necessary to consider the different Poisson ratios and have found considerable success in theoretical correlation of experimental data by taking all of the ν_{ij}, μ_{ij} as equal to zero (Refs. 15 and 16).

Hence, it is convenient, as well as meaningful to take in Eqs. (A. 8) and (A. 9) $\mu_{12} = \mu_{21} = \mu_{33} = \nu_{12} = \nu_{21} = \nu_{33} = \bar{\nu}$ the elastic Poisson ratio. Thus, it follows that

$$[m_1] = -[m_2] = \begin{vmatrix} 1 & \bar{\nu} & 0 \\ \bar{\nu} & 1 & 0 \\ 0 & 0 & (1-\bar{\nu}) \end{vmatrix} \qquad (A.11)$$

with

$$B_i = \frac{Et_i}{(1-\bar{\nu}^2)} \qquad \text{and} \qquad D_i = \frac{E I_i}{b_i(1-\bar{\nu}^2)}$$

for the elastic orthotropic case.

Plastic Isotropic Case: Here $\nu = 1/2$ and the plasticity coefficients A_{ij} appear.

$$[m_2] = -[m_1] \qquad [m_3] = [m_4] = 0$$

$$[m_1] = \begin{vmatrix} A_{11} & 1/2\ A_{12} & -1/2\ A_{13} \\ 1/2\ A_{12} & A_{22} & -1/2\ A_{23} \\ -1/2\ A_{13} & -1/2\ A_{23} & 1/2\ A_{33} \end{vmatrix}$$

with (A.12)

$$A_{11} = 1 - \alpha\,\sigma_x^2/4 \qquad A_{12} = A_{21} = 1 - \alpha\,\sigma_x\sigma_y/2$$

$$A_{22} = 1 - \alpha\,\sigma_y^2/4 \qquad A_{13} = A_{31} = 1 - \alpha\,\sigma_x\sigma_{xy}$$

$$A_{33} = 1 - \alpha\,\sigma_{xy}^2 \qquad A_{23} = A_{32} = 1 - \alpha\,\sigma_y\sigma_{xy}$$

where

$$\alpha = (3/\sigma_e^2)(1 - E_t/E_s)$$

Also,

$$B_i = 4E_s t/3 \qquad D_i = E_s t^3/9$$

Plastic Orthotropic Case: In a plastic orthotropic plate with symmetrical stiffening $[m_3] = [m_4] = 0$ and $[m_1] = -[m_2]$; $[m_1]$ has the same form as in the isotropic case [Eq. (A. 12)]. The rigidity terms are defined as follows:

$$B_i = 4E_s t_i/3 \qquad D_i = 4E_s t_i/3b_i$$

Governing Stability Equations

By utilizing the kinematic relations Eq. (A. 2), and the stress-strain relations, Eqs. (A. 6), it is possible to write the equilibrium equations, Eqs. (A. 1), in terms of the displacement components, u, v, w. The following equations are written for a cylinder (with $R_x = 0$ and $R_y = R$) which is elastic or plastic, isotropic or orthotropic. It is assumed that only in the plastic case, the external torsion loads (N_{xy}) are not applied in combination with the normal loads (N_x, N_y). In this case, $A_{13} = A_{23} = 0$. Assuming a symmetrical stiffening system, we find $[m_3] = [m_4] = 0$, $[m_2] = -[m_1]$ and

$$[m_1] = \begin{vmatrix} A_{11} & \bar{\nu} A_{12} & 0 \\ \bar{\nu} A_{12} & A_{22} & 0 \\ 0 & 0 & (1-\bar{\nu}) A_{33} \end{vmatrix} \qquad \text{(A. 13)}$$

$$B_i = \frac{\bar{E} t_i}{(1-\bar{\nu}^2)} \qquad D_i = \frac{\bar{E} I_i}{b_i (1-\bar{\nu}^2)}$$

Elastic: $\bar{\nu} = \nu$; $\bar{E} = E$

Plastic: $\bar{\nu} = 1/2$; $\bar{E} = E_s$

With these, the following are the equilibrium equations in terms of the displacement components u, v and w, after manipulating in the manner following Donnell.

$$\nabla_B^4 u = -\bar{\nu} \frac{A_{12}}{R} \frac{\partial^3 w}{\partial x^3} + \frac{A_{22}}{R} \left(\frac{B_2}{B_1}\right) \frac{\partial^3 w}{\partial x \partial y^2} \qquad \text{(A. 14)}$$

$$\nabla_B^4 \, v = -\frac{2}{R}\left[\frac{A_{11}A_{22}B_2}{(1-\bar{\nu})\,A_{33}B_3} - \frac{\bar{\nu}^2}{(1-\bar{\nu})}\frac{A_{12}^2 B_2}{A_{33}B_3} - \frac{\bar{\nu}}{2}A_{12}\right]\frac{\partial^3 w}{\partial x^2 \partial y} - \frac{A_{22}}{R}\left(\frac{B_2}{B_1}\right)\frac{\partial^3 w}{\partial y^3}$$

$$= -\frac{2}{R}\left[\frac{A_{11}A_{22}-\bar{\nu}^2 A_{12}^2}{(1-\bar{\nu})\,A_{33}}\left(\frac{B_2}{B_3}\right) - \frac{\nu}{2}A_{12}\right]\frac{\partial^3 w}{\partial x^2 \partial y} - \frac{A_{22}}{R}\left(\frac{B_2}{B_1}\right)\frac{\partial^3 w}{\partial y^3} \qquad (A.15)$$

$$\nabla_B^4\left\{A_1\frac{\partial^4 w}{\partial x^4} + 2\left[\frac{\bar{\nu}}{2}\,A_{12}\,\frac{(D_1+D_2)}{D_1} + (1-\bar{\nu})\,A_{33}\frac{D_3}{D_1}\right]\frac{\partial^4 w}{\partial x^2 \partial y^2} + A_2\left(\frac{D_2}{D_1}\right)\frac{\partial^4 w}{\partial y^4}\right.$$

$$\left. + \frac{N_x}{D_1}\,\frac{\partial^2 w}{\partial x^2} + 2\,\frac{N_{xy}}{D_1}\,\frac{\partial^2 w}{\partial x \partial y} + \frac{N_y}{D_1}\,\frac{\partial^2 w}{\partial y^2}\right\} + \frac{B_2}{R^2 D_1}\,(A_{11}A_{22}-\bar{\nu}^2 A_{12}^2)\frac{\partial^4 w}{\partial x^4} = 0 \qquad (A.16)$$

where ∇_B^4 is a differential operator given by

$$\nabla_B^4 = \frac{\partial^4}{\partial x^4} + 2\left[\frac{(A_{11}A_{22}-\bar{\nu}^2 A_{12}^2}{(1-\bar{\nu})\,A_{33}}\left(\frac{B_2}{B_3}\right) - \bar{\nu}\,\frac{A_{12}}{2}\,\frac{(B_1+B_2)}{B_1}\right]\frac{\partial^4}{\partial x^2 \partial y^2} + A_{22}\left(\frac{B_2}{B_1}\right)\frac{\partial^4}{\partial y^4} \qquad (A.17)$$

These equations together with the boundary conditions on u, v, w specify the complete solution of the problem. However, usually only conditions on w are used for the simply supported or clamped case;

Simply supported:	$w(0, L) = 0$	$\partial^2 w/\partial x^2\,(0, L) = 0$
Clamped:	$w(0, L) = 0$	$\partial w/\partial x\,(0, L) = 0$

This implies that certain constraints are placed on the u, v displacements.

Appendix 2

Solution for Compressive and Bending General Instability

Introduction

From Eq. (A.16) of Appendix 1 we have the governing equation for the stability of a cylinder including plastic and orthotropic effects. In this appendix we consider the case of an elastic orthotropic cylinder with symmetric stiffening, subject to compressive and bending loads.

Governing Equation

For an elastic cylinder, all the plasticity coefficients A_{ij} become equal to 1 or 0 and $\bar{\nu} = \nu$ the elastic Poisson ratio. Furthermore, the external load being axial both the N_{xy} and N_y terms disappear in Eq. (A.16). If we replace the x, y coordinates by an x, θ coordinate system, where θ represents the circumferential direction and x the axial direction, we have the following form for the governing equation:

$$\nabla_B^4\left\{\frac{\partial^4 w}{\partial x^4} + \frac{2}{R^2}\left[\nu/2\,(D_1+D_2)/D_1 + (1-\nu)\,D_2/D_1\right]\frac{\partial^4 w}{\partial x^2 \partial \theta^2} + D_2/D_1\,(1/R^4)\,\frac{\partial^4 w}{\partial \theta^4} + \frac{\bar{N}}{D_1}\,\frac{\partial^2 w}{\partial x^2}\right\}$$

$$+ (B_2/R^2 D_1)(1-\nu^2)\,\partial^4 w/\partial x^4 = 0 \qquad (B.1)$$

where

$$\nabla_B^4 = \partial^4/\partial x^4 + (2/R^2)\left[(1-\nu)\,B_2/B_3 - (\nu/2)(B_1+B_2)/B_1\right]\partial^4/\partial x^2 \partial \theta^2 + (B_2/B_1)(1/R^4)\,\partial^4/\partial \theta^4$$

If $\bar{N}$ the axial force term is due to compressive force $\bar{N} = N_c$ and if $\bar{N}$ is due to a pure bending moment, then $N = N_b \cos\theta$ where N_b is the maximum bending axial compressive force. Since the treatment in these cases is different they are best considered separately.

Compressive Stability

A very general asymmetric solution for Eq. (B.1) satisfying simple support conditions on w is obtainable by taking for w,

$$w = A_m \sin \frac{m\pi x}{L} \cos n\theta \qquad \text{(B. 2)}$$

where $n \geq 0$.

By treating m as a continuous variable and setting

$$\beta = \frac{nL}{m\pi R}$$

we obtain from Eq. (B. 1) utilizing Eq. (B. 2) the following expression for N_c:

$$\frac{N_c}{D_1} = \frac{m^2\pi^2}{L^2}\left[1 + 2\left\{\nu/2\,(D_1+D_2)/D_1 + (1-\nu)\,D_2/D_1\right\}\beta^2 + D_2/D_1\,\beta^4\right] + \left[(B_2/R^2D_1)(1-\nu^2)\right] L^2/\pi^2m^2\left[1 + 2\left\{(1+\nu)\,B_2/B_3 - \nu/2\,(B_1+B_2)/B_1\right\}\beta^2 + \frac{B_2}{B_1}\,\beta^4\right]^{-1} \qquad \text{(B. 3)}$$

Eq. (B. 3) may be further transformed to

$$k_c = m^2\left[1 + \frac{2\gamma\overline{\beta}^2}{\delta} + \frac{\alpha\overline{\beta}^4}{\delta}\right] + \frac{12Z^2(1-\nu^2)}{\pi^4}\left[1 + \frac{2\overline{\beta}^2}{\delta} + \frac{\overline{\beta}^4}{\delta}\right]^{-1}\frac{1}{m^2} \qquad \text{(B. 4)}$$

where:

$$\alpha = B_1D_2/B_2D_1$$

$$\gamma = \left[\nu/2\,(D_1+D_2) + (1-\nu)\,D_2\right]\left\{D_1\left[(1+\nu)\,B_2/B_3 - \nu/2\,(B_1+B_2)/B_1\right]\right\}^{-1}$$

$$\delta = (B_2/B_1s^2) \quad \text{with} \quad s = \left[(1+\nu)\,B_2/B_3 - \nu/2\,(B_1/B_2)/B_1\right]$$

$$\overline{\beta}^2 = \left(\frac{B_2}{B_1 s}\right)\beta^2 \qquad \text{(B. 5)}$$

$$k_c = \frac{N_c L^2}{\pi^2 D_1}$$

and $$12Z^2 = \frac{L^4B_2}{R^2D_1}$$

From Eq. (B. 4) we obtain axisymmetric and asymmetric solutions by letting β be equal to zero or otherwise.

Axisymmetric Solution: with $\beta = 0$, from Eq. (B.4) we have

$$k_c = m^2 + \frac{12Z^2}{\pi} (1-\nu^2) \frac{1}{m^2} \tag{B.6}$$

Treating m as a continuous parameter, this leads to the minimum solution

$$k_c = .702Z (1-\nu^2)^{1/2} \tag{B.7}$$

Asymmetric Solutions: From the general asymmetric form of Eq. (B.4) we can obtain two types of minima depending upon whether m is continuous or discrete. The lowest of the discrete solutions, of course, corresponds to m=1. Hence the asymmetric solutions are divided into m-continuous and m=1 cases.

Asymmetric m-continuous Solution: By treating m and β as continuous parameters in Eq. (B.4) we can minimize k_c with respect to m^2 and β^2. Using the stationariness requirement with respect to m^2 and β^2 we have the following two equations:

$$12 (1-\nu^2)\ Z^2/\pi^4\ (1/m^4) = \left[1 + 2\gamma\overline{\beta}^2/\delta + (\alpha/\delta)\overline{\beta}^4\right]\left[1 + 2\overline{\beta}^2/\delta + \overline{\beta}^4/\delta\right] \tag{B.8}$$

$$12 (1-\nu^2)\ (Z^2/\pi^4)(1/m^4) = \left[1 + 2\overline{\beta}^2/\delta + \overline{\beta}^4/\delta\right]^2 (\gamma + \alpha\overline{\beta}^2)/(1 + \overline{\beta}^2) \tag{B.9}$$

Solving Eqs. (B.8) and (B.9) we obtain for $\overline{\beta}^2$, the following:

$$\overline{\beta}^2 = \delta/2(\alpha-\gamma)\left[(1-\alpha) \pm \left\{(1-\alpha)^2 + (4/\delta)(1-\gamma)(\alpha-\gamma)\right\}^{1/2}\right] \tag{B.10}$$

Making use of Eqs. (B.8) and (B.9) in Eq. (B.4) we finally obtain:

$$k_c = .702Z (1-\nu^2)^{1/2}\ U \tag{B.11}$$

where

$$U = \left[(\gamma+\alpha\overline{\beta}^2)/(1+\overline{\beta}^2)\right]^{1/2} \tag{B.12}$$

Asymmetric m=1 Solution: In Eq. (B.4) if we let m=1 then

$$k_c = \left[1 + 2(\gamma/\delta)\overline{\beta}^2 + (\alpha/\delta)\overline{\beta}^4\right] + \frac{12Z^2(1-\nu^2)}{\pi^4}\left[1 + (2/\delta)\overline{\beta}^2 + \overline{\beta}^4/\delta\right]^{-1} \tag{B.13}$$

On minimizing this expression with respect to $\overline{\beta}^2$ we have:

$$k_c = \left[1 + 2\gamma\,(\overline{\beta}^2/\delta) + \alpha(\overline{\beta}^4/\delta)\right] + \left[1 + 2(\overline{\beta}^2/\delta) + \overline{\beta}^4/\delta\right](\gamma + \alpha\overline{\beta}^2)\,(1+\overline{\beta}^2)^{-1} \qquad \text{(B.14)}$$

and

$$12\,(1-\nu^2)\,Z^2/\pi^4 = \left[1 + 2(\overline{\beta}^2/\delta) + \overline{\beta}^4/\delta\right]^2 (\gamma + \alpha\overline{\beta}^2)\,(1+\overline{\beta}^2)^{-1} \qquad \text{(B.15)}$$

From these three possible modes, namely the axisymmetric, asymmetric m-continuous and asymmetric m=1, and the corresponding expressions for k_c from Eqs. (B.7), (B.11) and (B.14) we can determine the governing mode for given combinations of the orthotropic parameters α, γ, and δ. Of these parameters, δ is the least critical and for the most practical cylinders it is very close to unity.

Fig. 1 shows a γ-α chart in which the governing modes are shown for zones corresponding to certain α, γ combinations. Further details regarding the three solutions are to be found in Ref. 16.

Wavelengths in Axi- and Asymmetric Cases

In the solutions corresponding to Eqs. (B.7) and (B.11) where we have taken m as continuous and minimized the expressions with respect to m, the physical meaning of m large or continuous is that the wavelength λ in the axial direction which is given by L/m is small and can be treated as a continuous parameter. In the m=1 case, obviously, the wavelength is equal to the entire cylinder length.

From the above minimized expressions it is possible to write down the following relationships for the axial wavelengths (λ_x) in both the axi and asymmetric modes.

Thus, from Eq. (B.6)

$$\frac{\lambda^4_{axi}}{\pi^4} = \left[\frac{B_2(1-\nu^2)}{R^2 D_1}\right]^{-1} \qquad \text{(B.16)}$$

From Eq. (B.8) we have

$$\frac{\lambda^4_{asy}}{\pi^4} = \left[\frac{B_2(1-\nu^2)}{R^2 D_1}\right]^{-1} (1 + 2\gamma\overline{\beta}^2/\delta + \alpha\overline{\beta}^4/\delta)\,(1 + 2\overline{\beta}^2/\delta + \overline{\beta}^4/\delta) \qquad \text{(B.17)}$$

However, by equating Eqs. (B.8) and (B.9) we find

$$1 + 2\gamma\overline{\beta}^2/\delta + \alpha\overline{\beta}^4/\delta = U^2\,(1 + 2\overline{\beta}^2/\delta + \overline{\beta}^4/\delta) \qquad \text{(B.18)}$$

Hence,

$$\frac{\lambda^4_{asy}}{\pi^4} = \left[\frac{B_2(1-\nu^2)}{R^2 D_1}\right]^{-1} U^2 \left(1 + 2\bar{\beta}^2/\delta + \bar{\beta}^4/\delta\right)^2 \qquad (B.19)$$

From an examination of Eqs. (B.19) and (B.16) we see that the wavelength λ for axisymmetric case is obtained by setting $\beta = 0$ in Eq. (B.19) since this also leads to $U = 1$.

Hence, Eq. (B.19) represents a general expression for the wavelength in axi- and asymmetric cases. Utilizing Eq. (B.19) with (B.7) and (B.11) we can obtain the following general expression for N_c valid for both axi- and asymmetric m-continuous cases:

$$\frac{N_c \lambda^2}{\pi^2 D_1} = 2\, U^2 X^2 \qquad (B.20)$$

where $X^2 = (1 + 2\bar{\beta}^2/\delta + \bar{\beta}^4/\delta)$

In Eq. (B.20) $U \leq 1$, $X^2 \geq 1$ the equality holding for axisymmetric case.

Bending Stability

Referring back to Eq. (B.1) we take $\bar{N} = N_b \cos\theta$ where N_b is the maximum axial compressive loading due to an external bending moment M with $N_b = \frac{M}{\pi R^2}$ then we have the following governing equation for the bending stability:

$$L(w) \equiv \nabla_B^4 \left[\frac{\partial^4 w}{\partial x^4} + 2/R^2\ (\nu/2)(D_1 + D_2) + (1-\nu)D_3\ D_1\right]^{-1} \frac{\partial^4 w}{\partial x^2 \partial \theta^2} + (D_2/D_1)(1/R^4)\ \frac{\partial^4 w}{\partial \theta^4}$$

$$+ \frac{N_b}{D_1}\ \frac{\partial^2 w}{\partial x^2}\ \cos\theta\ + (B_2/R^2 D_1)\ (1-\nu^2)\ \frac{\partial^4 w}{\partial x^4} = 0 \qquad (B.21)$$

Since Eq. (B.21) has no direct solution satisfying the simple support condition on w, the Galerkin method is used to obtain the stability criterion.

In Ref. 17, it has been shown that, based upon the results of isotropic buckle pattern, the deflection function w can be represented by the following approximation.

$$w = A \sin \frac{m\pi x}{L} \cos N\theta \qquad |\theta| \leq \pi/2N$$
$$= 0 \qquad |\theta| > \pi/2N \tag{B.22}$$

where N is a fixed number greater than 1. It is shown in Ref. 17 that N is very much larger than unity.

Following the Galerkin procedure the stability equation is obtained by setting

$$\int_0^L \int_{\pi/2N}^{\pi/2N} L(w) \sin \frac{m\pi x}{L} \cos N\theta \; d\theta dx = 0 \tag{B.23}$$

Upon carrying out the indicated operation in Eq. (B. 23) we obtain as a result

$$k_b = \frac{\pi/2N}{\sin \pi/2N} (1 - 1/4N^2)\left[m^2\left\{1 + 2(\gamma/\delta)\,\overline{\beta}^{*2} + \frac{\alpha}{\delta}\,\overline{\beta}^{*4}\right\}\right.$$
$$\left. + \frac{12Z^2(1-\nu^2)}{\pi^4}\left\{1 + (2/\delta)\,\overline{\beta}^{*2} + \overline{\beta}^{*4}/\delta\right\}^{-1} (1/m^2)\right] \tag{B.24}$$

where $k_b = \dfrac{N_b L^2}{\pi^2 D_1}$ and $\overline{\beta}^{*2} = \left(\dfrac{B_2}{B_1}\right)\beta^{*2}$, with $\beta^* = \dfrac{NL}{m\pi R}$ (B. 25)

In Eq. (B. 25) α, γ, δ are the same orthotropic parameters as those defined in Eq. (B. 5).

Since the function $S(N) = \dfrac{\pi/2N}{\sin \pi/2N}(1 - 1/4N^2)$ very rapidly approaches 1 as N increases in value and since N is a fairly large number, Eq. (B. 24) finally reduces to:

$$k_b \simeq \left[m^2\left\{1 + 2(\gamma/\delta)\,\overline{\beta}^{*2} + (\alpha/\delta)\,\overline{\beta}^{*4}\right\}\right.$$
$$\left. + \frac{12Z^2(1-\nu^2)}{\pi^4}\left\{1 + 2/\delta\,\overline{\beta}^{*2} + \overline{\beta}^{*4}/\delta\right\}^{-1} (1/m^2)\right] \tag{B.26}$$

Eq. (B.26), for the bending case, is seen to be identical with that of the compressive case k_c from Eq. (B. 4) with the important difference that while β could become zero leading to an axisymmetric mode in the compressive case, β^* for the bending case can never equal zero. However, it may approach close to zero when terms like

$\overline{\beta}^{*2}$ and $\overline{\beta}^{*4}$ may be neglected. Hence in Eq. (B.26), upon neglecting terms multiplying $\overline{\beta}^{*2}$ and $\overline{\beta}^{*4}$, we can minimize the resulting expression with respect to m^2 and obtain a limiting solution as

$$k_b = .702Z\,(1-\nu^2)^{1/2} \qquad \text{(B.27)}$$

which is identical to the axisymmetric solution for the compressive case.

As for asymmetric solutions, the identity of forms for bending and compressive cases shows that we obtain the same stress results as in the compressive case. However, we have already seen that β^* is never equal to zero which implies that there is no true axisymmetric mode in the case of a bending problem.

Concluding Remarks

The behavior in the bending stability problem is generally governed by the fact that the external stress distribution changes from a compressive one at the top to a tensile one at the bottom half of a cross section of the cylinder. This precludes any buckling effect on the tension side. Hence, a compatible buckle pattern for the bending problem has to be deflection free on the tension side. Hence, a general type of asymmetric mode with ripples running all the way around the circumference, which is perfectly suitable in a compressive stability problem, becomes impossible in the bending case. A suitable pattern seems to have a single lobe symmetric about a vertical axis and whose maximum width is a small fraction of π which is signified by π/N, where N is usually a large number. Thus the buckling pattern presents a widely differing picture in the bending case as compared to the compressive case.

However, when we turn to the stress picture we find that for both the isotropic cylinders and for the orthotropic cylinders k_b/k_c is essentially equal to unity.

Appendix 3
Test Data on Stiffened Cylinders Under Compression

Introduction

Table 3.1 lists the groups of experimental data analyzed according to the orthotropic theory presented in Appendices 1 and 2. The data are grouped according to the references listed and include the range of orthotropic parameters pertinent to Fig. 1 on which they are displayed. Groups A, B, and C have previously been analyzed using the theory of Appendix 2 and the individual reference sources can be consulted for details of data reduction. Groups D, E, and F were analyzed in the present report using the theory of Appendix 2. Consequently, the overall methods of data reduction are discussed herein.

The total number of test points represent 63 orthotropic cylinders plus several isotropic cylinders which were used as control points to indicate the quality of the cylinder manufacturing and testing procedures. Cylinder diameters ranged from 6 to 120 in. with roughly 70 percent of 8 in. diameter. Test data for each group of data are individually displayed in Figs. 3.1 through 3.5; Groups E and F represent single test points and are listed in Table 3.1.

Reduction of Group D Data[20]

Calculations for the theoretical buckling under axial compressive loading of five longitudinally stiffened cylinders indicated by the data points in Fig. 3.5 followed methods presented in Refs. 11 and 16. These methods utilize three orthotropic parameters, α, γ, and δ which characterize the buckling behavior. Both γ and δ are a function of the effective shear thickness of the cylinder wall which was taken equal to the average of the sum of the cylinder cross sectional area per unit width in directions along and normal to the longerons (Ref. 16). The parameter γ is also a function of the cylinder wall unit torsional rigidity which was determined using the reference below.*

The range of values for the α, γ, δ parameters for the test specimens are presented in Table 3.1. Values for individual specimens were based on cylinder wall geometry in the buckle region and nominal values for the cylinder length and diameter as given in Ref. 20. All cylinders had values for α and γ indicating

*Becker, H., and Gerard, G., "Measurement of Torsional Rigidity of Stiffened Plates," NASA TN D-2007, July 1963.

Table 3.1

Orthotropic Cylinder Test Data Summary

Group	Reference	Cylinder Type	Diameter, in. and (no. specimens)	α	γ	δ	σ_{exp}/σ_x
A	(15) (16)	ring stiff. grid stiff.	8.0 (17)	1.5 - 10	$\simeq\alpha$	1.01 - 1.10	Fig. 3.1
A	(15) (16)	long. stiff. grid stiff.	8.0 (17)	0.13 - 0.70	0.91 - 1.07	1.01 - 1.10	Fig. 3.2
B	(18)	ring stiff.	8.0 (10), 24 (1), 84 (1)	3.0 - 21.0	1.25 - 1.95	1.02 - 1.05	Fig. 3.3
C	(19) (15)	filament wound	6.0 (5), 12 (2), 18 (2), 24 (1)	1.6 - 2.4	0.075 - 0.12	0.052 - 0.068	Fig. 3.4
D	(20)	long. stiff.	52 (5)	0.021 - 0.029	0.085 - 0.104	1.01 - 1.05	Fig. 3.5
E	(21)	truss-core sandwich	120 (1)	1.3	1.09	1.05	0.67
F	(22)	honeycomb sandwich	77 (1)	1.0	1.0	1.0	0.78

buckling in the asymmetric m=1.0 mode. The corresponding theoretical stress was determined using Ref. 16 and assuming ν=0.

The test specimens of Ref. 20 were instrumented with strain gages attached to the inside and outside skin as well as gages at stiffener locations. Test data show that the average stress in both the skin and stiffener was essentially equal up to failure. Values for the experimental stress used in the preparation of Fig. 3.5 correspond to the maximum average stress in the cylinder skin at specimen failure as indicated by the strain gage data.

Test data for orthotropic cylinders using a waffle configuration are also presented in Ref. 20. For these specimens, general instability failure was proceeded by local buckling of the skin between stiffeners. Because of this local buckling, the test results do not allow a valid evaluation of the general instability orthotropic theory and are not included. Results for two isotropic cylinders tested in Ref. 20, however, are shown in the figure.

Reduction of Group E Data[21]

As shown in Ref. 17, the theoretical elastic buckling stress of orthotropic cylinder under either bending or axial compression loading are equal; hence, tests on the general instability of cylinders in bending (such as Ref. 21) may be used to check axial compression orthotropic theory.

Values for the orthotropic parameters α, γ and δ for the truss-core sandwich cylinder of Ref. 21 are given in Table 3.1. In the calculation of these parameters, the shear thickness for the sandwich was calculated as described previously, and torsional stiffness parameters were determined using the reference below.* One observes that both α and γ have values greater than one which is indicative of buckling in the axisymmetric mode (Ref. 11).

As shown in Table I the experimental/theoretical buckling stress ratio for the specimen was 0.67. The theoretical buckling stress was calculated as 86.8 ksi based on average cross sectional geometry and using equations presented in Ref. 11 reduced for ν=0. The experimental peak failure stress was given in Ref. 21 as 58 ksi and was based on the maximum value for the average strain for the sandwich cross section as determined from strain measurements.

*Libove, C., and Hubka, R., "Elastic Constants for Corrugated-Core Sandwich Plates," NACA TN 2289, February 1951.

Reduction of Group F Data[22]

The buckling strength of honeycomb sandwich cylinders under bending loading was evaluated in Ref. 22, and the results for one cylinder which failed elastically is given in Table I, ($\sigma_{exp}/\sigma_x = .78$). For this specimen $\alpha=\gamma=\delta=1.0$ (see Table 3.1), and either the axisymmetric or asymmetric buckle mode governs (Ref. 11). Values for these parameters were based on calculations for the effective shear thickness as described previously and torsional stiffness relationships given in the reference below.* The theoretical buckling stress (65 ksi) was determined using nominal values for cylinder geometry and theoretical results presented in Ref. 11 reduced for $\nu=0$. The experimental buckling stress (50.4 ksi) was determined from strain gage data presented in Ref. 22 and corresponds to the average sandwich face stress at the extreme fibre from the cylinder neutral axis.

*Cheng, S., "Torsion of Sandwich Panels of Trapezoidal, Triangular, and Rectangular Cross Sections," Forest Products Laboratory Rept. No. 1874, June 1960.

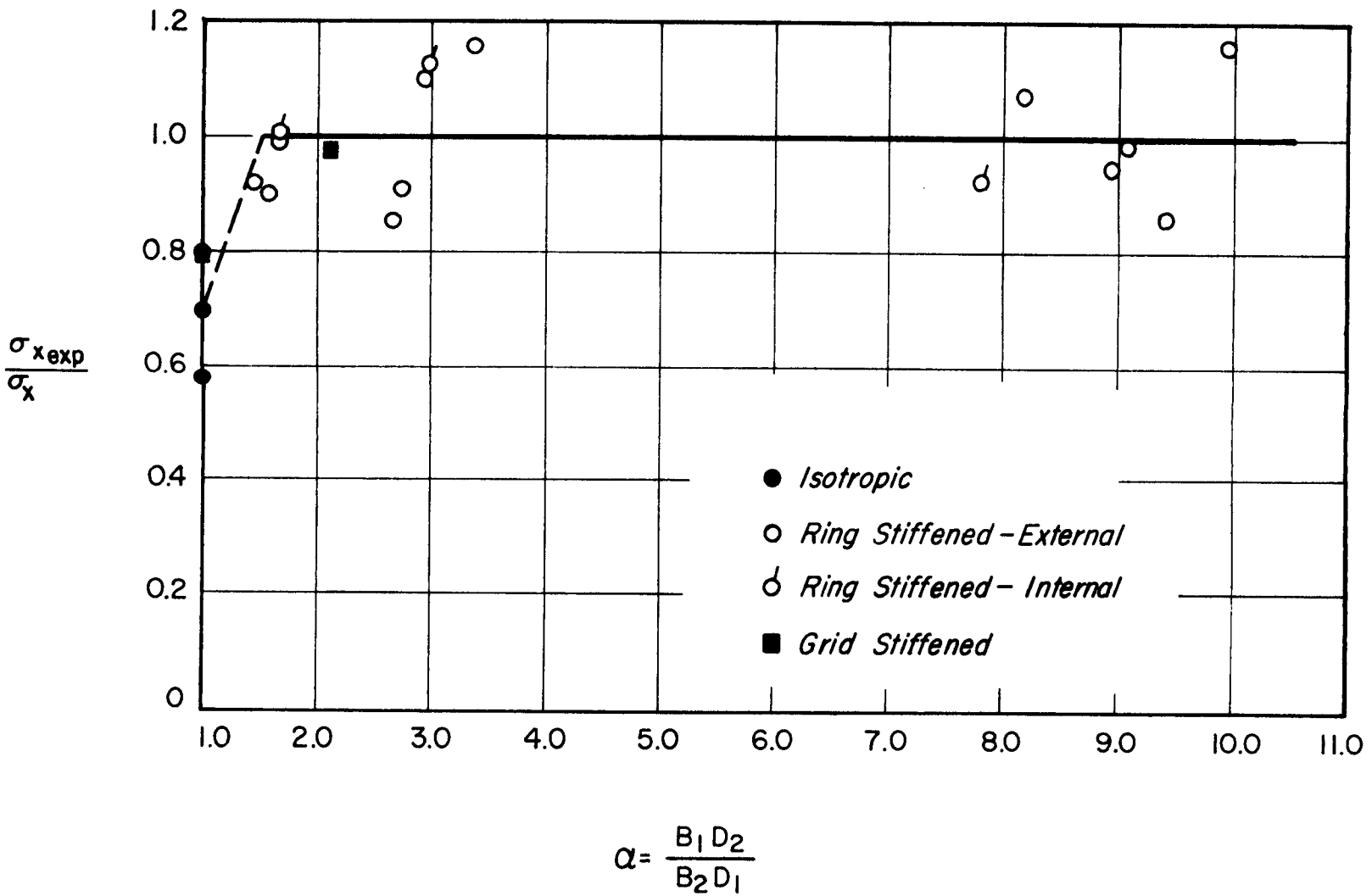

Figure 3.1 Stress ratio for ring stiffened cylinders under compression, Group A.

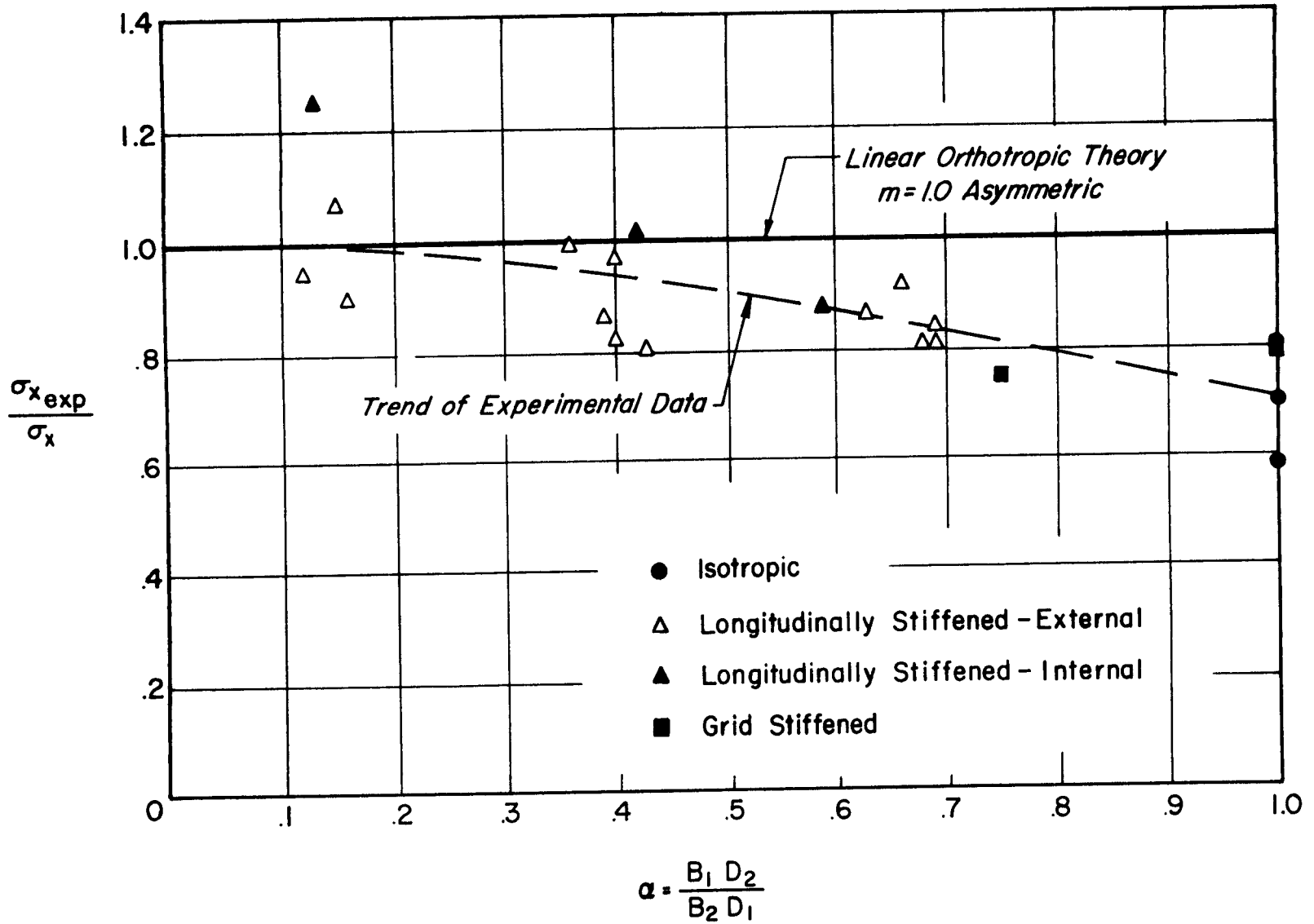

Figure 3.2 Stress ratio for grid and longitudinally stiffened cylinders under compression, Group A.

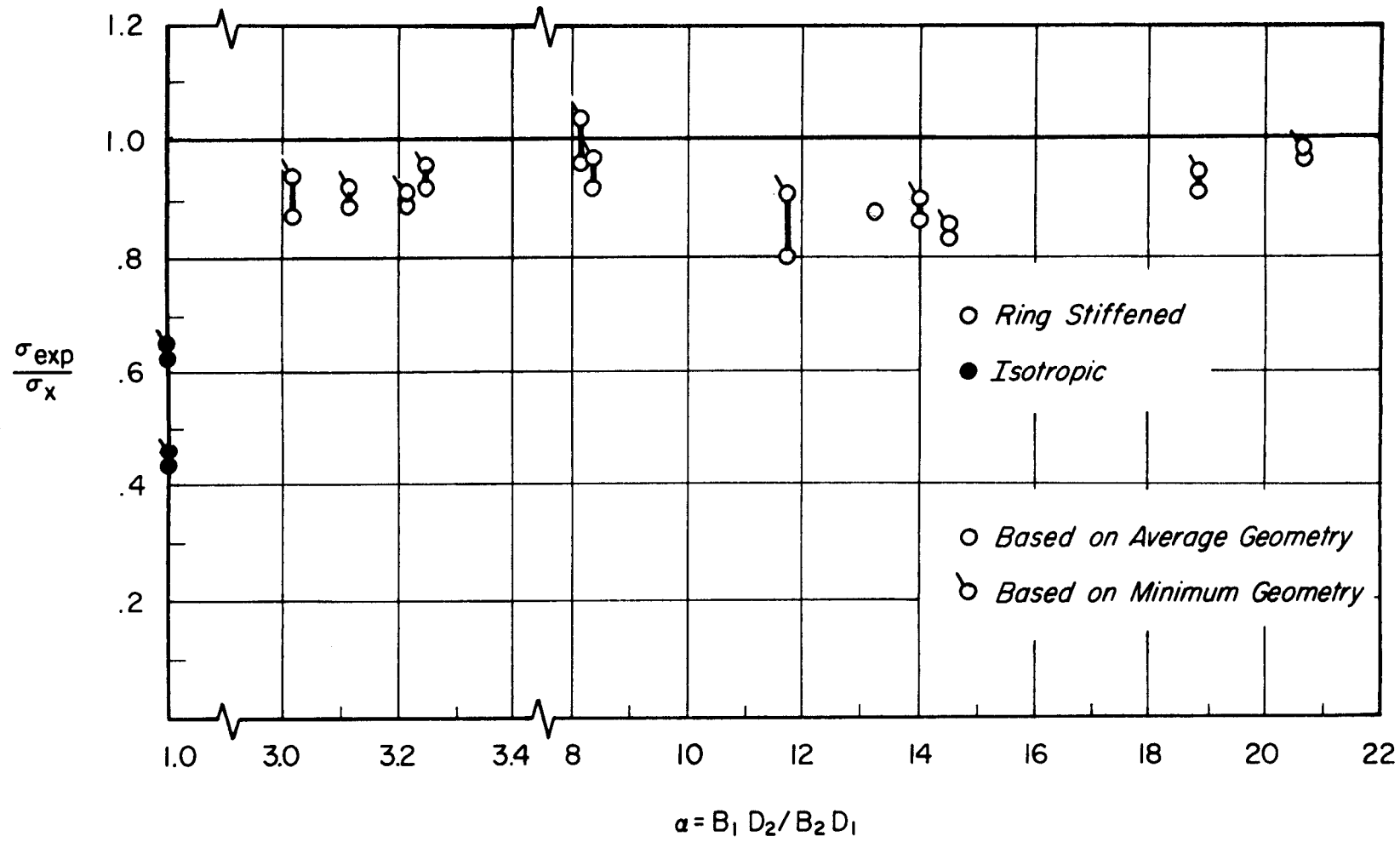

Figure 3.3 Stress ratio for ring stiffened cylinders under compression, Group B.

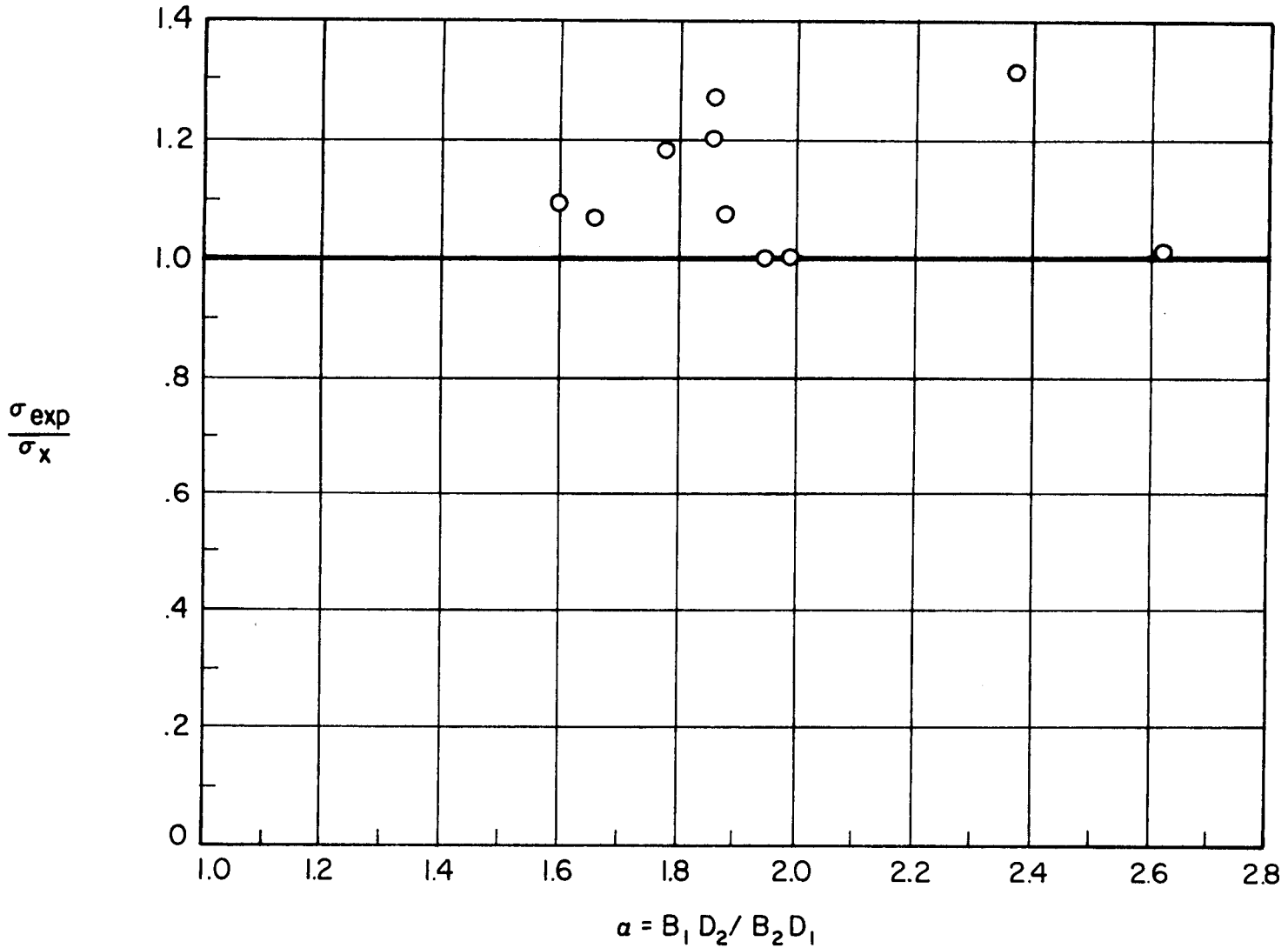

Figure 3.4 Stress ratio for filament wound cylinders under compression, Group C.

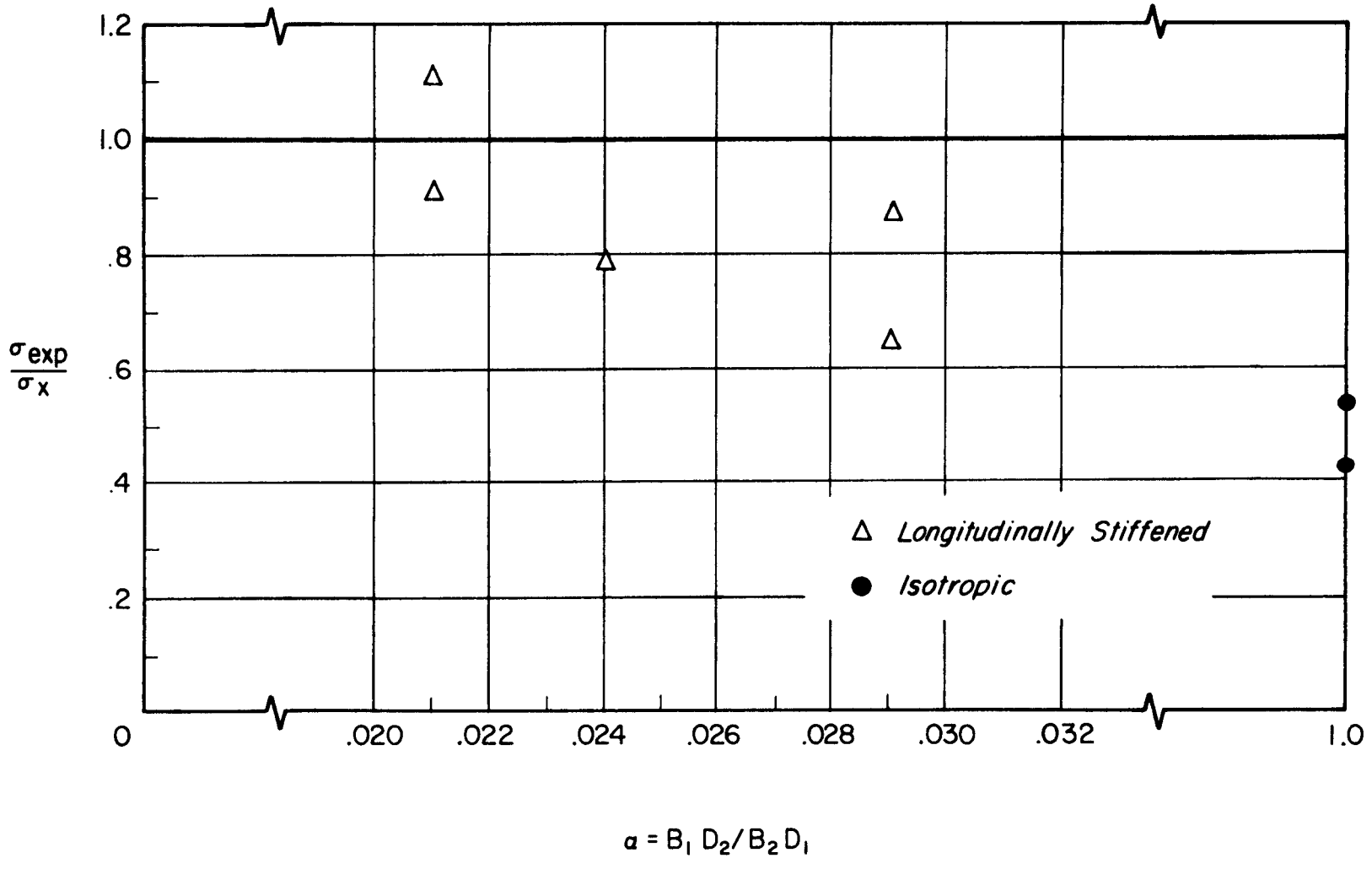

Figure 3.5 Stress ratio for longitudinally stiffened cylinders under compression, Group D.